Energy, Mines and Resources Canada
Earth Physics Branch
1 Observatory Crescent
Ottawa Canada
K1A 0Y3

Energie, Mines et Ressources Canada
Direction de la physique du globe
1 Place de l'Observatoire
Ottawa Canada
K1A 0Y3

Geothermal Service of Canada

Service géothermique du Canada

HEAT FLOW STUDIES IN THE SOHM ABYSSAL PLAIN AND THEIR RELEVANCE TO NUCLEAR WASTE DISPOSAL INVESTIGATIONS.

M. Burgess and A. Judge

pp. including figures

Price/Prix: $19.80

Earth Physics Branch Open File No. 81-15

Ottawa, Canada, 1981

ABSTRACT

In June 1980 geothermal investigations were conducted in a 10 km x 10 km flat study area in the southern Sohm Abyssal Plain, western North Atlantic Ocean. These measurements formed part of a major oceanographic expedition, on board the C.S.S. Hudson, to study the nature of abyssal plain sediments and their suitability for hosting implanted canisters of nuclear waste. The geothermal programme investigated the thermal characteristics of the sediments: their thermal properties and temperature gradients. 450 thermal conductivity measurements on retrieved sediment cores range from .74 to 2.12 $Wm^{-1}\ K^{-1}$, averaging $1Wm^{-1}K^{-1}$. Sediment temperature gradients range from 35.0 to 68.4 mKm^{-1} and average 54.4 mKm^{-1} for 6 gradiometer probe penetrations. Sediment temperature profiles are non-linear indicating perturbations to the thermal regime, such as vertical convection of interstitial waters or changes in bottom water temperature, may exist.

RESUME

Au mois de juin 1980 une recherche géothermique fut entreprise sur une superficie de 10km x 10km dans la plaine abyssale de Sohm, au nord-ouest de l'Océan Atlantique. Cette étude ne constituait qu'une partie d'une expédition océanographique majeure pour étudier le caractère des sédiments de la plaine abyssale et pour juger s'ils seraient convenables pour l'entreposage des récipients de déchêts nucléaires. Le programme géothermique fut établi pour déterminer les caractéristiques thermiques des sédiments: leur propriétés thermiques et leur gradients de température. Les 450 mesures de conductivité thermique prises sur les carottes de sédiments varient de 0.74 à 2.12 $Wm^{-1}K^{-1}$, avec une moyenne de 1 $Wm^{-1}K^{-1}$. Le gradient thermique dans les sédiments varie de 35.0 de 35.0 à 68.4 mKm^{-1}, avec une moyenne de 54.4 mKm^{-1} sur 6 mesures. Les profils de la température dans les sédiments ne sont pas linéaires. Ceci indique un régime thermique perturbé, par exemple par des changements dans la température de l'eau du fond ou par la circulation des eaux interstitielles.

TABLE OF CONTENTS

1. INTRODUCTION

The possible disposal of high level nuclear waste products in deep sea sediments has recently received international and national attention. Six nations, through the coordination of the North Eastern Atlantic (NEA) Seabed Working Group are undertaking deep sea geological investigations to determine the nature of abyssal plain sediments and to study their suitability for hosting implanted canisters of nuclear waste. Canada as a member nation, has a programme of investigation consisting of 4 designated tasks (Buckley, 1981); 1) to determine seabed geomorphology and surficial geology, 2) to determine physical properties of pelagic sediments, 3) to determine geochemical properties and reactivities of pelagic sediments, and 4) to determine sediment dynamics at selected sites.

In June 1980 a major oceanographic expedition was undertaken to investigate the geological and geochemical characteristics of the southern Sohm Abyssal Plain, Western North Atlantic Ocean (Fig. 1). This cruise, conducted from the CSS Hudson (based at Bedford Institute of Oceanography, Dartmouth, N.S.) was the only site investigation carried out by any member nation of the Working Group in the Western North Atlantic in 1980. The Sohm Abyssal Plain experiment involved seismic profiling and surficial sediment sampling, sedimentological, geotechnical, geochemical and geothermal analyses. The geochemical investigations were designed to examine the partition and movement of selected elements whose behaviour may simulate that of the radioactive elements which would ultimately escape from a corroded or leaking nuclear waste canister. Several parameters were studied: mineralogy of sediments, water content, organic carbon, redox conditions and rates of chemical diffusion of elements through the sediment column.In addition the

experiments were designed to look for evidence of water movement within the sediments; such movement could bring radioactive materials into contact with the water column.

The Geothermal Studies group of the Earth Physics Branch of E.M.R. was invited to undertake the preliminary geothermal analyses in the Sohm Abyssal Plain. The effect of high temperatures developed in and around the deposited waste canisters must be determined. Using the thermal properties of the sediments and the nature of the heat source (radioactive isotopic composition, isotopic levels and the distribution of canisters) the temperature and temperature gradient distribution can be determined, thus the integrity of the system. The geothermal programme was designed to investigate the thermal characteristics of the sediments: their thermal properties and temperature gradients. The gradients are used to examine the natural environment for presence of natural advection. Four hundred and fifty thermal conductivity measurements were performed on retrieved sediment cores to depths of over 12m and six temperature-depth profiles were measured in the sediments to depths of over 5m. Departures from linearity in the geothermal profiles may help to detect horizontal or vertical fluid movements within the sediments. Non-linear geothermal profiles may be fitted to vertical conduction-convection models and an estimate of vertical fluid velocities may be obtained (Bredehoeft and Papadopulos, 1965; Anderson, Hobart and Langseth, 1979; Mansure and Reiter, 1979). These velocities may then be compared to estimates obtained from pore water chemistry profiles determined on core samples (Crowe and McDuff, 1979). Geothermal measurements thus provide additional information relevant to the examination of the movement of elements through the sediment and water column.

Thermal gradients reflect the general stability of the deep sea floors. Several sources of perturbation to the temperature field in the sediments may exist other than the circulation of interstitial waters. These include topographic variations of the sea-bottom, active sedimentation or erosion of surface sediments, variable bottom water currents, large bottom water temperature gradients, short and long-term changes in bottom water temperature, and spatial contrasts in the thermal conductivity of sediments (Langseth et al., 1966; Lubimova et al., 1965).

This report presents and briefly discusses the results of the thermal measurements conducted during the Sohm Abyssal Plain (SAP) cruise (Hudson 80-016). A literature search to compile available heat flow and related data in the surrounding section of the Northwestern Atlantic Ocean and to describe the physiography, geology and oceanography of the SAP area was first conducted to provide a useful framework for the data analysis.

2. PHYSIOGRAPHY, GEOLOGY AND OCEANOGRAPHY OF THE SOHM ABYSSAL PLAIN (largely from Emery and Uchupi, 1972).

The SAP covers an area of 908,000 km^2 and is larger than the sum of all the other abyssal plains in the Western North Atlantic Ocean. The western margin of the T-shaped plain lies at a depth of 5000m, the eastern margin at 5150m. The centre of the cross bar reaches depths of 5400m while in the south, along the main arm of the T, depths reach 5600m. The plain then becomes unrecognizable among the Abyssal Hills (general bathymetry is shown in Fig. 7). Outlying members of the New England Seamount Chain (late Mesozoic to early Cenozoic in age), rising to 1250m and flanking the western arm of the T, occur in the Sohm Basin and are gradually being buried. The Northeast

Channel, the deep sea channel that begins on the continental shelf between Georges Bank and Nova Scotia, terminates at the left end of the T. The right end of the T is the terminus of the Northwest Atlantic Mid Ocean Canyon which drains southward along the west side of Greenland. These two channels provide the sediment source for the basin. The Hudson 80-016 study area is located in the southern distal portion of the plain in water depths of over 5300m (Fig. 1) The depth of oceanic basement in the SAP is greater than 6 km; a blanket of sediments 1-2 km thick covers the plain. Fig. 2 indicates the age of oceanic rock beneath the Northwestern Atalntic; 100 my basement underlies the study area.

The surface sediments of silty clay, clay minerals consisting of 60-80% illite, have settled from suspension in the sea water. They are interbedded with deposits of fine sand and silt from turbidity currents occurring every several hundred to several thousand years. These turbidity currents travel down channels in the continental slope and rise to dump transported material on the plain. Larger amounts of sand and silt are thus present in the plain than on the slopes or rises. During the last 10,000 years turbidity currents have been much less active. The rising sea level since the Pleistocene Epoch has not allowed transport and accumulation of sand from the now submerged beaches into the heads of the canyons; smaller volumes of sediments were trapped, hence less instability and less slumping.

Water contents of the sediments are typically 50-100% dry weight corresponding to bulk densities of 1.52 - 1.45 gcm^{-3}. Shear strengths vary from 35 -70 gcm^{-3} (higher in clay); the top meter of many deep sea cores is commonly overconsolidated. Estimated rates of deposition of sediment, or more properly rates of accumulation since erosion may remove some, vary from 0.3 to 5 cm/1000 yr for the Holocene deposits on the abyssal plains.

Several bodies of water underlie the surface waters of the Western North Atlantic. Temperature-salinity diagrams for these masses are presented in Fig. 3. Characteristics of these masses are listed below, from the surface downwards.

i) Western North Atlantic Water lies from the surface seasonally mixed layer down to the 4°C isotherm (when underlain by Meriterranean water it only extends down to the 10°C isotherm). The Gulf Stream and associated currents are part of this mass.

ii) Mediterranean Water is traced from the Straits of Gibraltar westward and south of the Azores, across the mid Atlantic Ridge. This water mass occurs in the southern portion of the Sohm Abyssal Plain.

iii) North Atlantic Deep Water contains 70% of all North Atlantic water colder than 4°C and arises from the mixing of Arctic, Antarctic, and Mediterranean waters.

iv) Norwegian Sea Overflow water, colder and fresher than iii), contains waters from various northern areas of extreme cooling flowing past Iceland and Greenland to continue southwestward.

v) Antarctic Bottom Water flows slowly northward along the sea floor. The top of the layer is the 1.8°C potential isothermal surface. Movement of this water mass over large areas of the deep sea floor with which it is in contact, coupled with temperature changes throughout geologic time (e.g. cooling resulting from Pleistocene glaciation) has probably had an effect on the thermal regime of the bottom sediments. However flow is slower than that of vi) and current features on the bedding plane are probably restricted.

vi) Western Boundary Undercurrent is a continuation of iv), moving southward along the western side of the ocean and possibly extending into several different water masses.

The highest salinities, greater than $36.6^{o}/oo$ are found in the warmer Mediterranean waters (>15°C). Salinities in the colder water masses range from $36^{o}/oo$ (15°C) to less than $35^{o}/oo$ in the very cold (<1°C) Antarctic Bottom Water.

Bottom water temperature and temperature gradient information in the Sohm Abyssal Plain area is included in Appendix A. Bottom water temperatures recorded range from 1.7 to 2.2°C, the coldest occurring in the deepest waters of the Sohm Abyssal Plain. No attempt has been made to look at the seasonal or periodic variability of the bottom water temperature data. The few bottom water potential temperature gradients measured range from $< 1 \times 10^{-2}$ to $3 \times 10^{-1} mKm^{-1}$. The adiabatic gradient in deep ocean water is $1.3 \times 10^{-1} mKm^{-1}$ (Lubimova et al., 1965). Where near-bottom water temperature gradients are much in excess of adiabatic, i.e. super-adiabatic, gravitational fluid instability is implied. This instability leads to convective overturn in the bottom water which in turn produces a sediment water interface temperature variable in time. Langseth et al (1966) found that large temperature gradients are associated with the upper boundary of the Antarctic Bottom Water. Where this boundary is close to the sea floor, large variations of bottom water temperature with time are thus possible. Heat flow may thus be disturbed by transients. In Fig. 4, showing water temperature profiles in the Sohm Abyssal Plain, the upper boundary of the Antarctic Bottom Water is at a depth of less than 3000m and does not appear close to the sea floor, suggesting stability of the bottom water temperature.

3. HEAT FLOW DATA LITERATURE SEARCH

A grid extending roughly from 43° to 60°W and 25° to 40°N was selected for the search. In addition to the Sohm Abyssal Plain, the Abyssal Hills, the Mid Atlantic Ridge and the Bermuda Rise which fall within the literature search grid, data from stations outside the grid in the Hatteras and Nares Abyssal Plains have been included. Data of interest at a site consisted of heat flow, water depth, thermal conductivity of sediments and thermal gradients in sediments, nature of sediments, bottom water temperatures and temperature gradients, non-linearity in gradients if noted, interval of sediments over which heat flow was determined and corrections, if any, applied to heat flow calculations. Data has been compiled in tabular form in Appendix A and listed according to physiographic unit. The location of the stations in the grid and the heat flow determined at each are plotted in Fig. 5. The thermal conductivities at these heat flow sites and the distribution of surface sediments in the area are shown in Fig. 6. Fig. 7 maps the bathymetry of the Sohm Abyssal Plain and shows the sediment temperature gradients measured at the heat flow sites as well as a few bottom water temperatures.

The main source of this data is the World Heat Flow Data Collection (Jessop et al., 1976) which provides a listing of all terrestrial and oceanic data to 1974. Since 1974 most surveys in the Northwestern Atlantic have focused on the Bermuda Rise and the Reykjanes Ridge (R.P. von Herzen, pers. comm.). Whenever possible the original reference for each heat flow site was consulted for additional information. When this reference was not verified, the stations are annoted by * in the listing.

A paucity of data exist for the SAP. Seven heat flow stations lying in the main arm of the T or bordering it have an average heat flow of

36.5 mWm^{-2}, with values ranging widely from 19.7 to 60.7 mWm^{-2} in similar water depths. The average heat flow for the basins of the Northwest Atlantic is approximately 48 $mWm^{-2} \pm 10$ (Langseth et al., 1966). Studies in the Nares and Hatteras Abyssal Plain by Reitzel (1963) indicated a very uniform heat flow for this basin averaging 47.7 mWm^{-2} over 16 stations. More recent studies in the Nares Abyssal Plain (Embley et al., 1979) have delineated very high heat flow anomalies with heat flow rising to 764 mWm^{-2} from 63 mWm^{-2} over a 600m wide dome. Several other closely spaced measurements in the Nares plain varied little from 63 mWm^{-2}.

Surface sediments in the SAP are largely clayey or sandy silt. A belt of clay extends across the basin above the southern arm of the T. The predominantly sandy surface sediments over the Seamount chain extend slightly into the plain. Thermal conductivities measured in the SAP are relatively uniform ranging from .70 to .96 $Wm^{-1}K^{-1}$. Temperature gradients in the sediments vary from 21.9 to 62 mKm^{-1}. This wide range of temperature gradients is responsible for the wide range of calculated heat flow values.

The measured sediment temperatures, from which the gradients were calculated, were not listed in most references. When these data were available, an examination of the sediment temperature profile revealed non-uniform sediment temperature gradients with depth in roughly half the cases. This non-uniformity was occasionally commented upon (e.g. Lister and Reitzel, 1964) and some of its possible sources discussed. Most often the mean gradients were merely listed with no indication as to uniformity or non-uniformity with depth.

4. GEOTHERMAL MEASUREMENTS, HUDSON CRUISE 80-016, SOHM ABYSSAL PLAIN

The study of the nature of Abyssal Plain sediments and their suitability for hosting high level nuclear waste disposal canisters

necessitates both regional and detailed small scale variability surveys. For the latter purpose a 10 x 10 km flat study area, in water depths of 5367m, was selected in the southern SAP following an initial seismic survey of the sea bottom. Within the study grid (cf Fig. 5 for location), which extended from longitude 55°55.0'W to 56° 01.4'W and latitude 32° 26.2'N to 32° 33.2N, sampling stations were randomly generated. General details on the surveying, sampling, subsampling techniques and analyses performed on board ship are summarized in the cruise report (Report of Cruise No. 80-016, CSS. Hudson, May 26 - June 27, 1980). Five heat flow stations for a total of six gradiometer probe penetrations to depths of over 5m were successfully occupied on the cruise (Fig. 8). Thermal conductivity measurements were made on retrieved core samples for a total of 450 determinations. In addition, a Time Domain Reflectometry (TDR) technique (Patterson and Smith, 1981) was used to measure experimentally the volumetric water content of the sediments and hence to evaluate the application of the technique to measurements in saline soils.

4.1. Equipment

Sediment temperature gradients were measured with a TR 12 gradiometer probe. This Bullard type probe (Langseth, 1965) measures the temperature of equally spaced sensors (thermistors) installed in an oil filled tube which is thrust into the ocean bottom. Digitized data is logged internally on a 6.4 mm. magnetic tape recorder: the entire electronics section is housed in an aluminum cylinder capable of recording in water depths greater than 4 km. The TR 12 is completely self-contained and programmable, allowing selection of sample time, digitization resolution and number of thermistors to be scanned. Two probe configurations were employed on the cruise, each with 7 sensors:

i) 3m long, 1.6 cm diameter, 40 cm sensor spacing.

ii) 5m long, 2.5 cm diameter, 80 cm sensor spacing.

Sensors were scanned every 12 seconds with a resolution of 2 mK.

Sediment thermal conductivity measurements were made using the transient needle probe technique (Von Herzen and Maxwell, 1959). A very thin needle (1mm diameter, 64mm long) inserted into the sediment core is heated by an internal heater wire (50Ω) at a known and constant rate (100 mA). The rate of rise of the temperature of the sensor situated at the centre of the needle is a function of the thermal conductivity of the soil. A plot of temperature versus the logarithm of time enables the calculation of thermal conductivity. Several needle probes were attached in series on the Hudson cruise enabling more than one measurement to be made during a run. Temperatures were recorded every 20 seconds for 7 minutes with a resolution of 1 mK. Thermal conductivity measurements were made on all cores (except one reserved for geotechnical purposes) at an average spacing of 15 cm. Retrieved cores were immediately stored vertically in a cold room to preserve as closely as possible bottom water temperature conditions and the thermal conductivity measurements were made prior to further analyses.

4.2 Results

Thermal conductivity profiles have been plotted at each core sampling stations. These, along with tables listing the conductivities, are compiled in Appendix B and a histogram is plotted in Fig. 9a. The tables also list the mean conductivity of the core as well as the harmonic mean conductivity. All measurements have been corrected to sea bottom water temperatures and pressures (Ratcliffe, 1960; MacDonald and Simmons, 1972). Thermal conductivities ranged from .74 to 2.12 $Wm^{-1}K^{-1}$ and averaged 1.06 $Wm^{-1}K^{-1}$.

Bottom water temperatures at the SAP heat flow stations ranged from 2.1 to 2.2°C. The frictional heat of penetration of the gradiometer probe disturbs the equilibrium sediment temperatures. The probe is thus left in the sediments for 20-25 minutes to monitor the decay in the temperature disturbance. A plot of the temperatures for each sensor as a function of inverse time and an extrapolation to infinite time yields the equilibrium temperature. Temperature-depth profiles at the stations are plotted in Appendix C. Sediment temperatures are referenced to the sediment-water interface and are given in millidegrees (mK); sensors are equally and accurately spaced, however the exact position of the interface above the top sensor is determined by extrapolation of the temperature gradient of the uppermost sensors. A listing of temperature gradients calculated by a least squares fit to all temperature points is included in Appendix C. The gradients range from 35.0 to 68.4 mKm^{-1} and average 54.4 mKm^{-1}.

5. Discussion

5.1 Thermal Conductivities

There are two features to note on the thermal conductivity plots aside from a slight trend towards increasing conductivity with depth typical in ocean bottom sediments. The very high conductivities encountered at the base of the piston cores correspond to coarse sediment deposited by a major turbidite from the Grand Banks. This event whose source has been confirmed by the heavy minerals, coal and fossils present in the cores, has a maximum date of 2Ma (D. Buckley, pers. comm.). The coarse sandy layers contain more siliceous detrital material and are hence more thermally conductive than the finer mud or clay layers. The second notable feature is the occasional high

conductivity encountered throughout a core (e.g. station 24). A radiographic profile of piston core 50 shows an excellent correlation between these higher conductivities and the bases of turbidite sequences (D. Buckley, pers. comm.). The increase in particle size at the base of the sequence and the corresponding increase in more thermally conductive detrital material is sufficient to raise the thermal conductivity from 1 to 1.4 $Wm^{-1}K^{-1}$. That this correlation occurred at all is merely an accident of the spacing of the conductivity measurements. A different spacing may not have sampled these higher conductivity intervals, which may explain why these are not observed in all cores.

A separate estimate of the thermal conductivities may be made from the sediment water contents. Ratcliffe (1960) showed that conductivities of deep ocean sediments depend more on their water contents than on the solid phase constituents and prepared nomograms for assessing the conductivity from the water content. Using Ratcliffe's determination and the measured water contents of the Sohm cores thermal conductivities were estimated. Water contents determined by K. Moran, U. of Rhode Island, on subsamples selected from the same interval as the needle probe measurement were used to calculate the thermal conductivity. Water contents were also determined by the Atlantic Geoscience Centre, but since their sampling interval differed these were not used in the conductivity calculations. Fig. 9b is a histogram of all 270 water content measurements; values ranged from 10 to 90% wet weight.

Conductivities calculated from water contents in nearly all cases were lower than those measured by the needle probe technique (e.g. Fig. 10). Since the depth of the needle probe measurement and the water content determination do not always exactly coincide, individual comparisons are

difficult; they do indicate that water content estimates may be from 5 to 35% lower than direct needle probe measurements. In general for a core, the mean of the estimated values is 16% lower than the mean of the measured values. It is likely that Ratcliffe's relationship, which was determined from measurements on red clays, does not apply to the Sohm sediments. The presence, variation in grain size and amount of detrital material in the SAP suggests that the composition of the solid phase constituents is an important factor in determining thermal conductivity and is overlooked when estimating conductivity from water contents.

5.2 Gradients

Several temperature profiles in Appendix C show a departure from linearity which is concave downwards. The frictional heat of penetration of the gradiometer probe is the greatest at the tip of the probe. Hence sensors closer to the tip require the longest time to settle to equilibrium temperatures. The non-linearity in the temperature profiles might then be due to non-equilibrium of the probe's deeper sensors. A close examination of the plots of temperature versus time for each sensor at each station indicates that the probe has been held in the bottom for a sufficient time to allow an extrapolation to equilibrium temperatures to be made. The trends, as the probe settles towards equilibrium, differ little from one sensor to the next.

When there are no perturbations to the geothermal regime and heat flow is by conduction only, temperature-depth plots will be linear providing thermal conductivity is constant with depth. Concavity in the Sohm profiles could be a reflection of increased conductivity with depth. To verify whether the non-linearity in the Sohm profiles is due to conductivity variations a

Bullard plot (Bullard, 1939) was drawn for each station. This is a plot of the temperature versus the integrated thermal resistance (calculated using the thermal conductivities from the closest coring stations) to the depth of measurement. The slope of the plot, the heat flow, should be linear if heat flow is constant with depth. The Bullard plots for the SAP, included in Appendix C along with a listing of heat flow calculated from a least squares fit to all points, essentially maintain the same non-linearity. Thus perturbations to the geothermal profile can not be accounted for by the variations in conductivity observed.

As mentioned in the introduction many sources of perturbations exist. Preliminary analysis of the SAP profile, assuming the non-linearity to be due solely to vertical convection of interstitial waters, suggests that circulation velocities on the order of 80-200 cm/year may be present in the sediments. Plots of temperature gradient versus temperature (e.g. Fig. 11 station 44) were fitted to vertical conduction-convection models (Mansure and Reiter, 1979) in which linearly increasing gradients with increasing temperature are indicative of downwards flow, decreasing gradients of upwards flow and constant gradients, no flow. Both upwards and downwards circulation may be occurring at some locations. The zones where changes in the flow regime appear to occur do not seem to correspond to lithological changes in the sediment column - e.g. to the presence of sand stringers. However the sediment grain size analyses reported in Buckley (1981) were performed over large intervals of core and were not continuous throughout the core. Hence zones of sand stringers may have been overlooked; the radiographic profile of piston core 50 indeed revealed many zones of silt lamina. Comparison of the thermal conductivity profiles with the apparent zones of change in

interstitial water circulation reveals some correlation with higher thermal conductivities (3 out of 6 cases). This would suggest the presence of coarser material over these intervals.

The fit of the non linear geothermal profiles to vertical conduction-convection models however does not preclude the possibility that other sources of perturbation to the thermal regime may exist. Step changes in bottom water temperatures may result in similar non-linear profiles. In Fig. 12 the temperature gradient versus temperature plot for 3 months after a 50 mk increase in bottom water temperature (for a sediment with an initial temperature gradient of 55 mKm^{-1} and a diffusivity of $2 \times 10^{-7} m^2 s^{-1}$) has been compiled using the relation derived by Carslaw and Jaeger (1959, pp 58-61) to determine the change in temperature gradient with depth. A fit of this data to vertical conduction-convection models yields velocities of the same order of magnitude as those interpreted from the Sohm data.

The stability of the bottom water temperatures in the SAP needs to be ascertained; slight seasonal fluctuations could create some of the observed non-linearities in the geothermal profiles. Large vertical temperature gradients in the near-bottom could lead to gravitational instability near the bottom and possible convective overturn of the water producing a temperature variable in time at the sediment-water interface (Langseth et al., 1966). Variable currents at the sea floor could also produce a variable rate of heat exchange with the sea floor and thus a variable effective temperature at the sea floor (Lubimova et al., 1965). Unfortunately attempts to record current rates at 50m and 150m above bottom, during Hudson cruise 80-016, proved unsuccessful when both current meters flooded.

The heat flow is also influenced by large scale and small scale (10's of meters) topographic changes in the sea bottom. Topographic corrections

often need to be applied. A correction to take into account the rate of sedimentation might also be required; rapid sedimentation results in a blanketing effect with heat flow in sediment filled pockets being depressed from regional values. Decreasing heat flow with depth could also be indicative of erosion of near-surface sediments. The heat flow-age of the ocean floor relationship (heat flow proportional to $t^{-1/2}$, t =age of the sea floor) proposed by Parsons and Sclater (1977) can be used indirectly to examine local processes perturbing the heat flow. Using this relationship a heat flow value of 47 mWm^{-2} is predicted for the 100 my old basement underlying the Sohm study area. Parsons and Sclater however point out that for ages greater than 80 my the relationship needs to be tested more stringently. Average heat flow determined from the Sohm gradiometer stations is 53.7 mWm^{-2}. Corrected heat flow values may also be used to test further the application of amino acid racemization rates in the determination of heat flow (Bada and Man, 1980).

5.3 Recommendations

Future investigations to determine the nature of abyssal plain sediments and their suitability for hosting implanted canisters of nuclear waste might benefit from the following considerations.

1) Closely spaced needle probe thermal conductivity measurements may yield lithological information before splitting and/or sectioning a core and thus help to decide on the type and frequency of subsampling for subsequent analysis (e.g. geochemical).
2) The stability of the sea bottom water temperature should be monitored (for 6 months - 1 year) by installing a thermograph recorder and sensor cables on and immediately above the sea bottom. Current meters might also be emplaced at the same time.

3) Heat flow gradiometer stations should be made to coincide as closely as possible with a coring station, these were often more than 1 km apart on Hudson cruise 80-016. Similarly core samples should at least cover the same depth interval probed by the gradiometer. One method of overcoming these problems would be to mount temperature sensors on the piston core barrels, ensuring that conductivity and temperature measurements coincide. This equipment is however delicate, costly, and cannot yield the precisions possible with a Bullard probe.

4) An increase in the number of temperature sensors and a decrease in their spacing would permit a better definition of gradient changes, i.e. of the shape of the geothermal profile, and thus would help to define the sources of disturbances in the profile and to discriminate better between possible processes of thermal perturbation.

5) Telemetry of data to surface either acoustically or along a cable and immediate reduction could identify critical areas for closely spaced detailed observations.

ACKNOWLEDGMENTS

We would like first to thank Vic Allen of the Earth Physics Branch, EMR for his superior assistance, during the Sohm cruise, in the maintenance and preparation of the geothermal equipment, in the needle probe thermal conductivity measurements and in the data reduction. We also thank Dale Buckley, Gus Vilks and Dave McKeown of the Bedford Institute for their efficient organization of the cruise and their cooperation. Finally we thank the crew of the CSS Hudson as well as the scientific crew for all their help. The geothermal investigations were funded by the Atlantic Geoscience Centre, Bedford Institute of Oceanography, Dartmouth, N.S.

REFERENCES*

Anderson, R.N., M.A. Hobart and M.G. Langseth. 1979 Geothermal Convection Through Oceanic Crust and Sediments in the Indian Ocean. Science, 204, 828-832.

Bada, J.L. and E.H. Man. 1980. Amino acid diagenesis in Deep Sea Drilling project cores: kinetics and mechanisms of some reactions and their applications in geochronology and in paleo-temperature and heat flow determinations. Earth-Science Review, 16, 21-55.

1. Birch, F.S. 1965. Heat Flow near the New England Seamounts. J. Geophys. Res., 70, 5223-5226.

2. Birch, F.S. and A.J. Halunen 1966. Heat Flow Measurements in the Atlantic Ocean, Indian Ocean, Mediterranean Sea and Red Sea. J. Geophy. Res., 71, 583-586.

3. Bookman, C.A., I. Malone and M.G. Langseth. 1973. Sea Floor Geothermal Measurements from Vema Cruise 26. Columbia Univ. Tech. Rept., 7 - CU-7-73.

Bredehoeft, J.D. and I.S. Papadopulos. 1965. Rates of vertical groundwater movement estimated from the earth's thermal profile. Water Resour. Res., 1, 325-328.

Buckley, D. 1981. "Canadian Report to Site Assessment Task Group" Proceedings of the Sixth Annual Meeting NEA Seabed Working Group, Paris, France, Feb. 2-5, 1981 (in preparation; a Sandia Laboratory Report).

Bullard, E.C. 1939. Heat flow in South Africa. Proc. Roy. Soc. London, A, 1973, 474-502.

Carslaw, H.S. and J.C. Jaeger. 1959. Conduction of heat in solids. 2nd ed. Oxford Univ. Press, London, 58-61.

Crowe, J. and R.E. McDuff. 1979. Temperature and pore water chemistry profiles of sediments in the Equatorial Pacific: Incompatible results? (abstract), EOS, 60(46), P. 863.

4. Embley, R.W., M.A. Hobart and R.N. Anderson 1979. A very high heat flow anomaly over 80 M.Y. old Atlantic Ocean floor. (abstract) EOS, 60, 155:18, p.383.

Emery, K.O. and E. Uchupi. 1972. Western North Atlantic Ocean. Topography, Rocks, Structure, Water, Life and Sediments. AAPG, 532 pp.

5. Gerard, R., M.G. Langseth and M. Ewing, 1962. Thermal gradient measurements in the water and bottom sediment of the Western Atlantic. J. Geophys. Res., 67, 785-803.

*Numbers are references used in compiling Appendix A.

Herzen, R. von and A.E. Maxwell, 1959. The measurement of thermal conductivity of deep sea sediments by a needle probe method. J. Geophys. Res., 64(10), 1557-1563.

6. Herzen, R. von and G. Simmons. 1972. Two heat flow profiles across the Atlantic Ocean. Earth Planet. Sci. Let., 15, 19-27.

7. Hobart, M.A., G.B. Udinstev and A.K. Popova. 1974. Heat flow measurements in the East-Central Atlantic Ocean and near the Atlantic Fracture Zone. In Problems of Oceanic Rift Zone, Ed. A.P. Vinogradov et al., Nauka Press, Moscow.

Jessop, A.M., M.A. Hobart and J.G. Sclater. 1976. The World Heat Flow Data Collection -1975. Geothermal Series Number 5, Geothermal Service of Canada, Energy, Mines and Resources, Canada, 125 pp.

Langseth, M.G. 1965. Techniques of measuring heat flow through the ocean floor. In Terrestrial Heat Flow, W.H.K. Lee Ed., Geophysical Monograph Series 8, AGU, 58-77.

8. Langseth, M.G., X. LePichon and M. Ewing. 1966. Crustal structure of the Mid-ocean ridges. 5. Heat flow through the Atlantic Ocean Floor and convection currents. J. Geophys. Res. 71, 5321-5355.

9. Langseth, M.G., I. Malone and D. Breger. 1970. Sea floor geothermal measurements from Vema Cruise 25. Columbia Univ. Tech. Rept. 2-CU-2-2-70, 168 pp.

10. Langseth, M.G., I. Malone and C.A. Bookman. 1972. Sea floor geothermal measurements from Vema Cruise 25. Columbia Univ. Tech. Rept. 4-CU-4-72, 163 pp.

11. Lister, C.P.B. and J.S. Reitzel 1964. Some measurements of Heat Flow through the Floor of the North Atlantic. J. Geophys. Res. 69, 2151-2154.

Lubimova, E.A., R.P. von Herzen and G.B. Udintsev. 1965. On heat transfer through the Ocean Floor. In Terrestrial Heat Flow, W.H.K. Lee Ed., Geophysical Monograph Series 8, AGU, 78-86.

MacDonald, K. and G. Simmons. 1972. Temperature coefficient of the thermal conductivities of ocean sediments. Deep-Sea Res., 19, 669-671.

Mansure, A.J. and M. Reiter. 1979. A vertical groundwater movement correction for heat flow. J. Geophys. Res. 84, B7, 3290-3496.

12. Nason, R.D. and W.H.K. Lee. 1964. Heat flow measurements in the North Atlantic, Caribbean and Mediterranean. J. Geophys. Res., 69, 4875-4883.

Parsons, B. and J.G. Sclater. 1977. An analysis of the variation of ocean floor bathymetry and heat flow with age. J. Geophys. Res., 82, 803-827.

Patterson, D.E. and N.W. Smith. 1981. The measurement of unfrozen water content by time domain reflectometry; results from laboratory tests. Can. Geotech. J., 18, 131-144.

Ratcliffe, E.H. 1960. The thermal conductivity of ocean sediments. J. Geophys. Res., 65(5), 1535-1541.

13. Reitzel, J.S. 1963. A region of uniform heat flow in the North Atlantic. J. Geophys. Res., 66., 2267-2268.

Report of Cruise No. 80-016, C.S.S. Hudson, May 26-June 27, 1980. D.L. McKeown, Ed., Bedford Institute of Oceanography, Dartmouth, Nova Scotia.

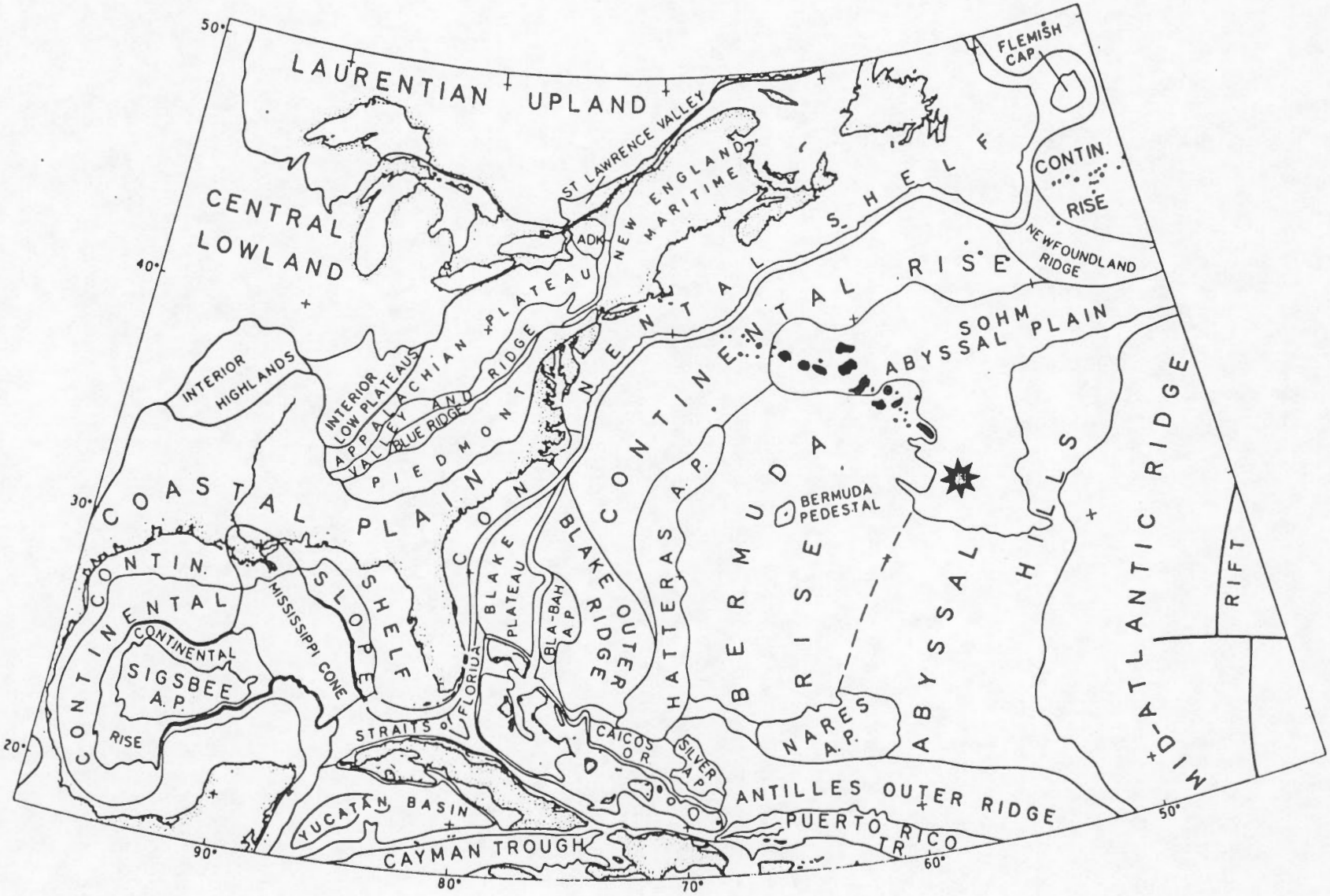

Fig. 1. Physiographic units of the Northwestern Atlantic.

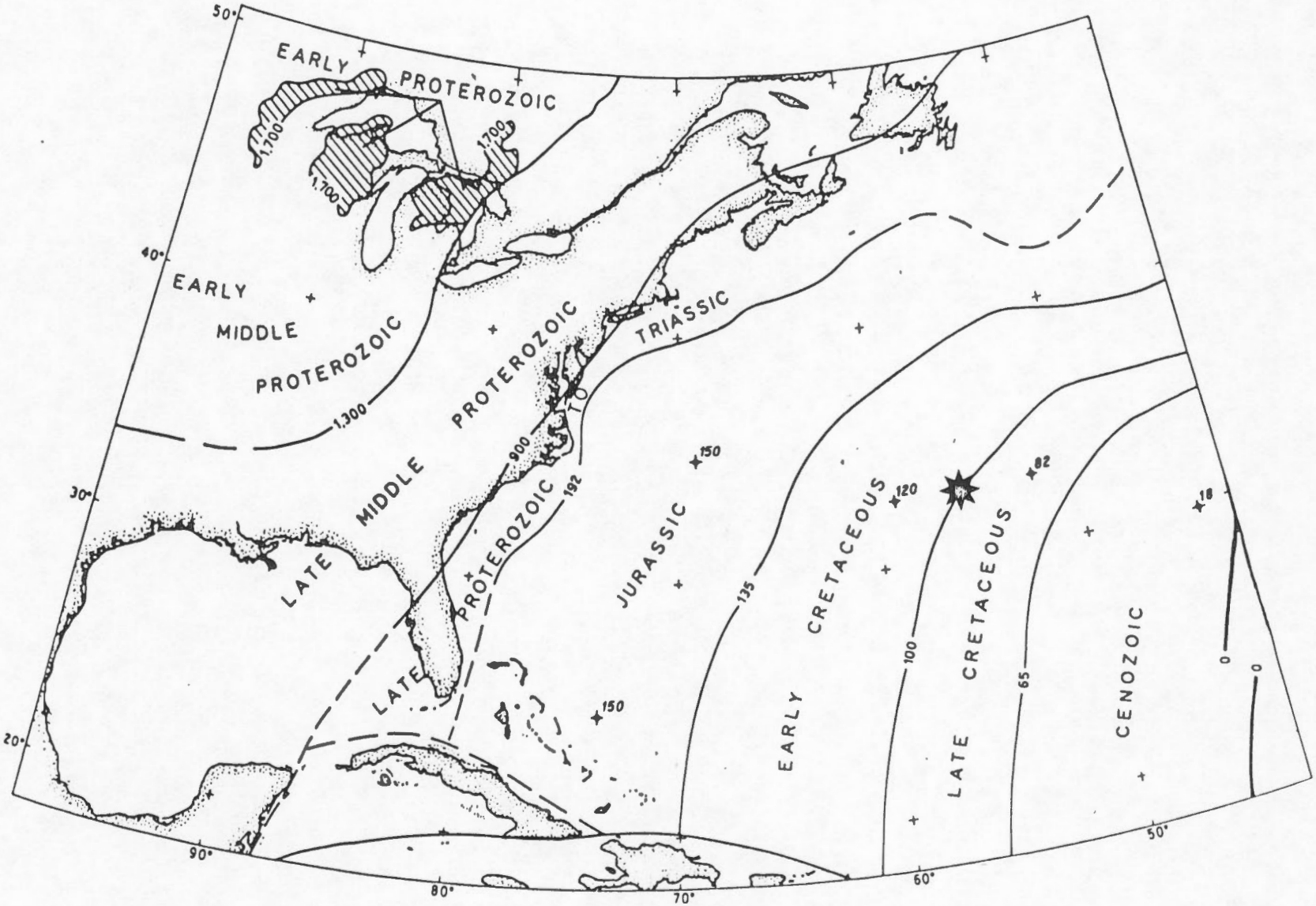

Fig. 2. Age (million years) of basement rocks, Northwestern Atlantic.

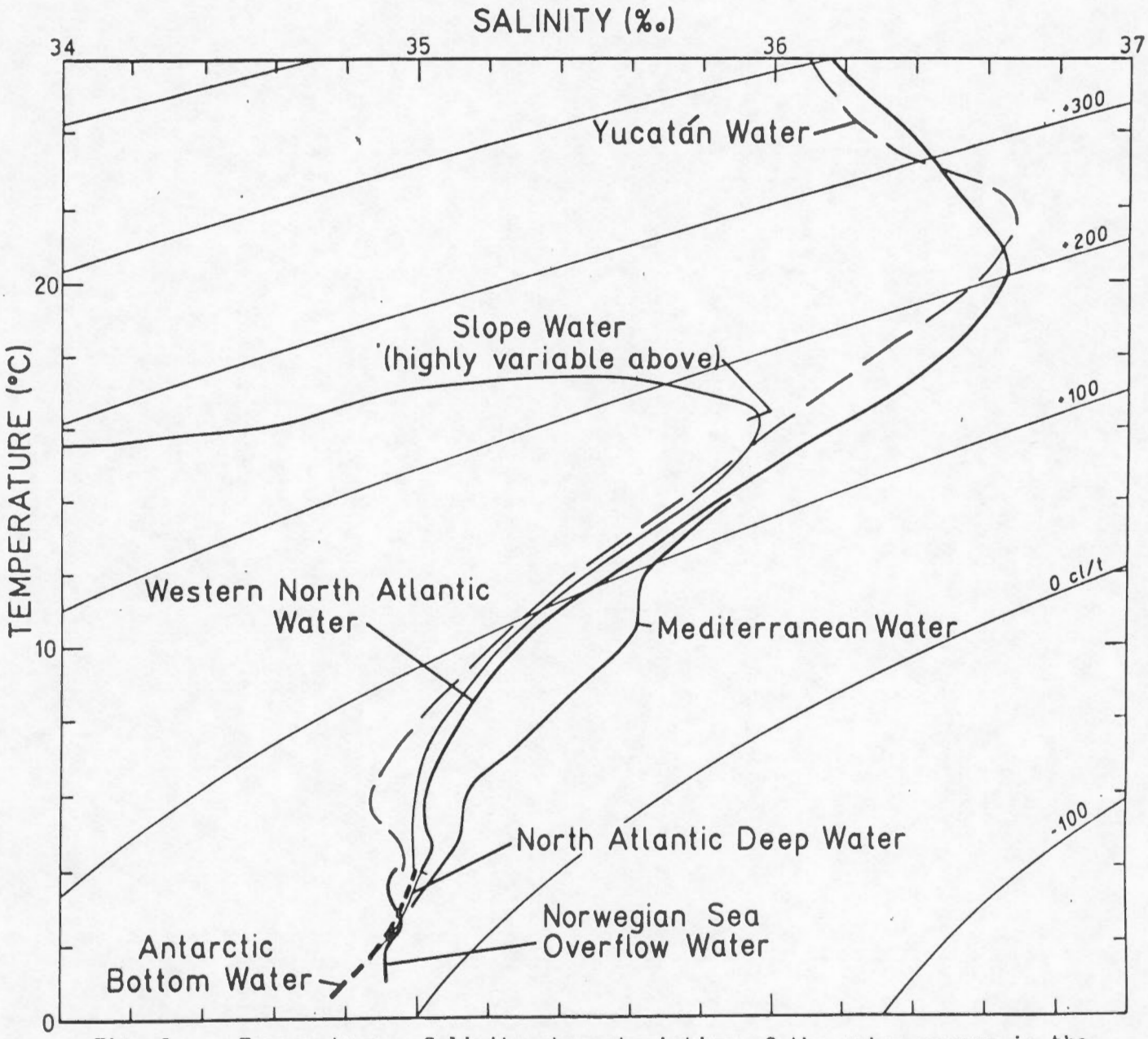

Fig. 3. Temperature - Salinity characteristics of the water masses in the

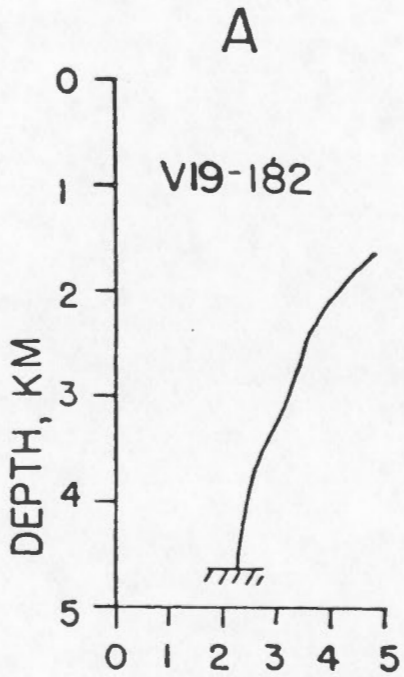

Fig. 4.a) Water temperature profile near the Sohm Abyssal Plain (33.18°N, 48.16°W).

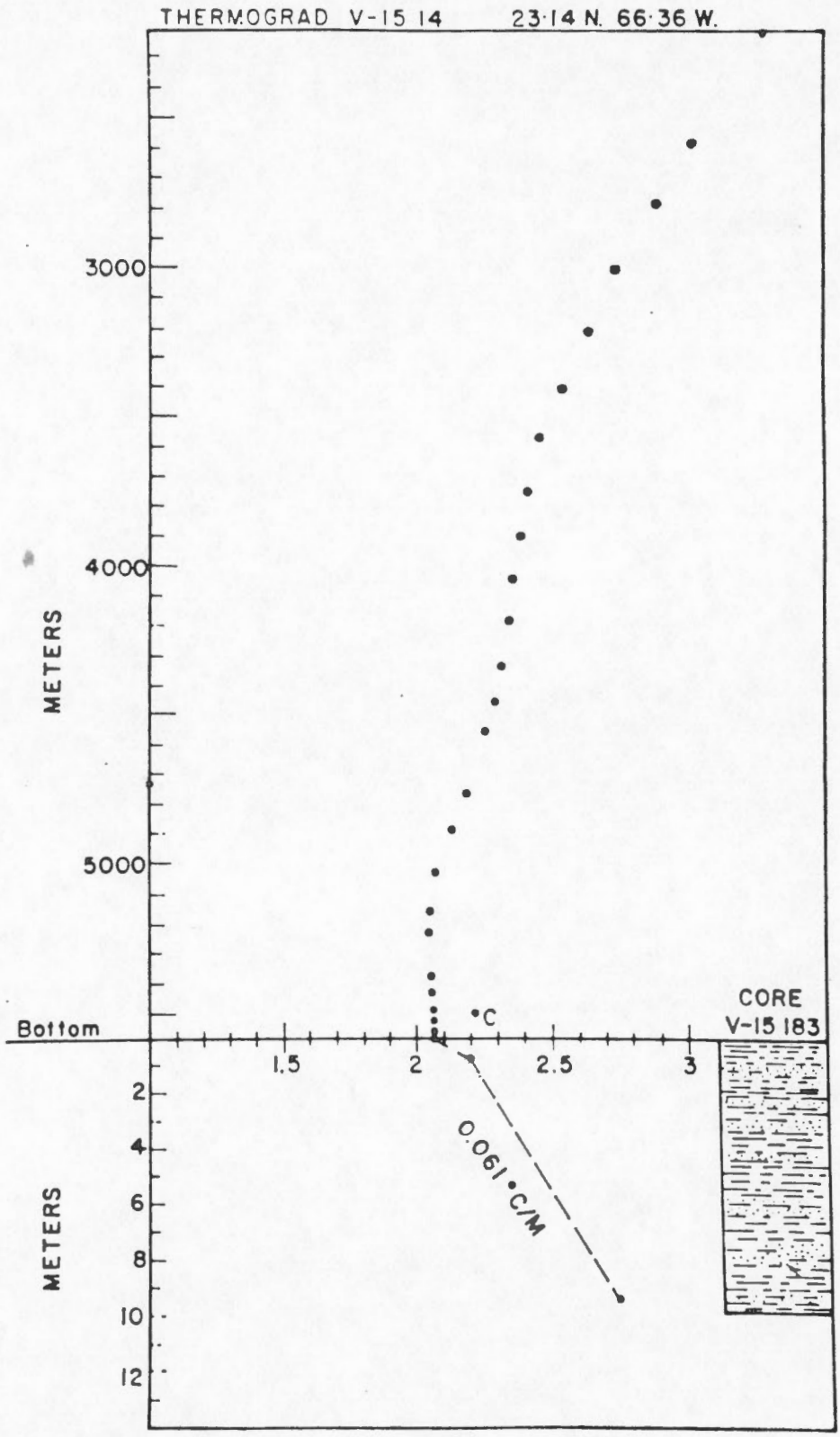

Fig. 4.b) Water temperature profile in the Nares Abyssal Plain (23.14°N, 66.36°W).

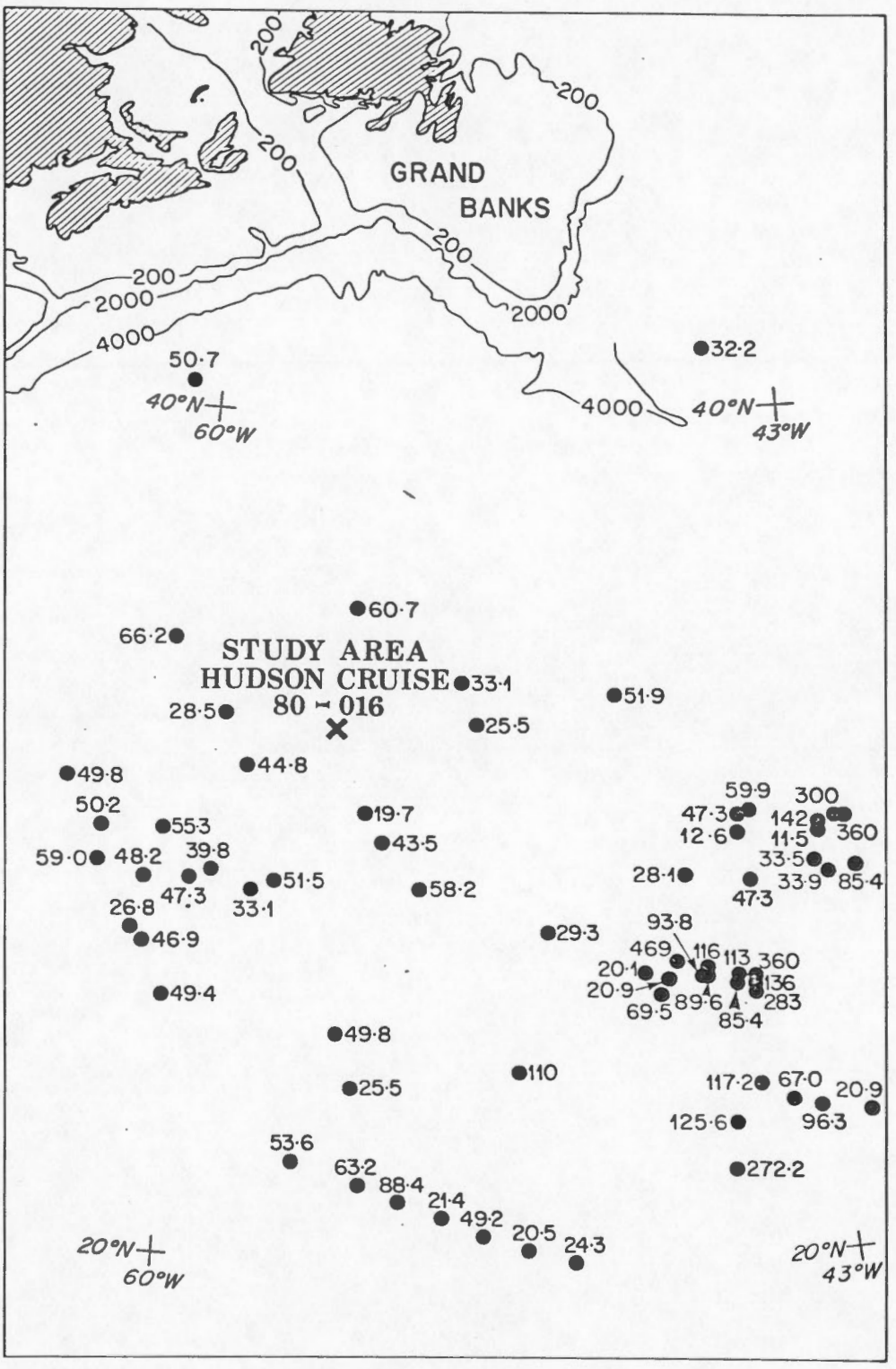

Fig. 5. Heat flow (mWm^{-2}), Northwestern Atlantic Ocean, Sohm Abyssal Plain area.

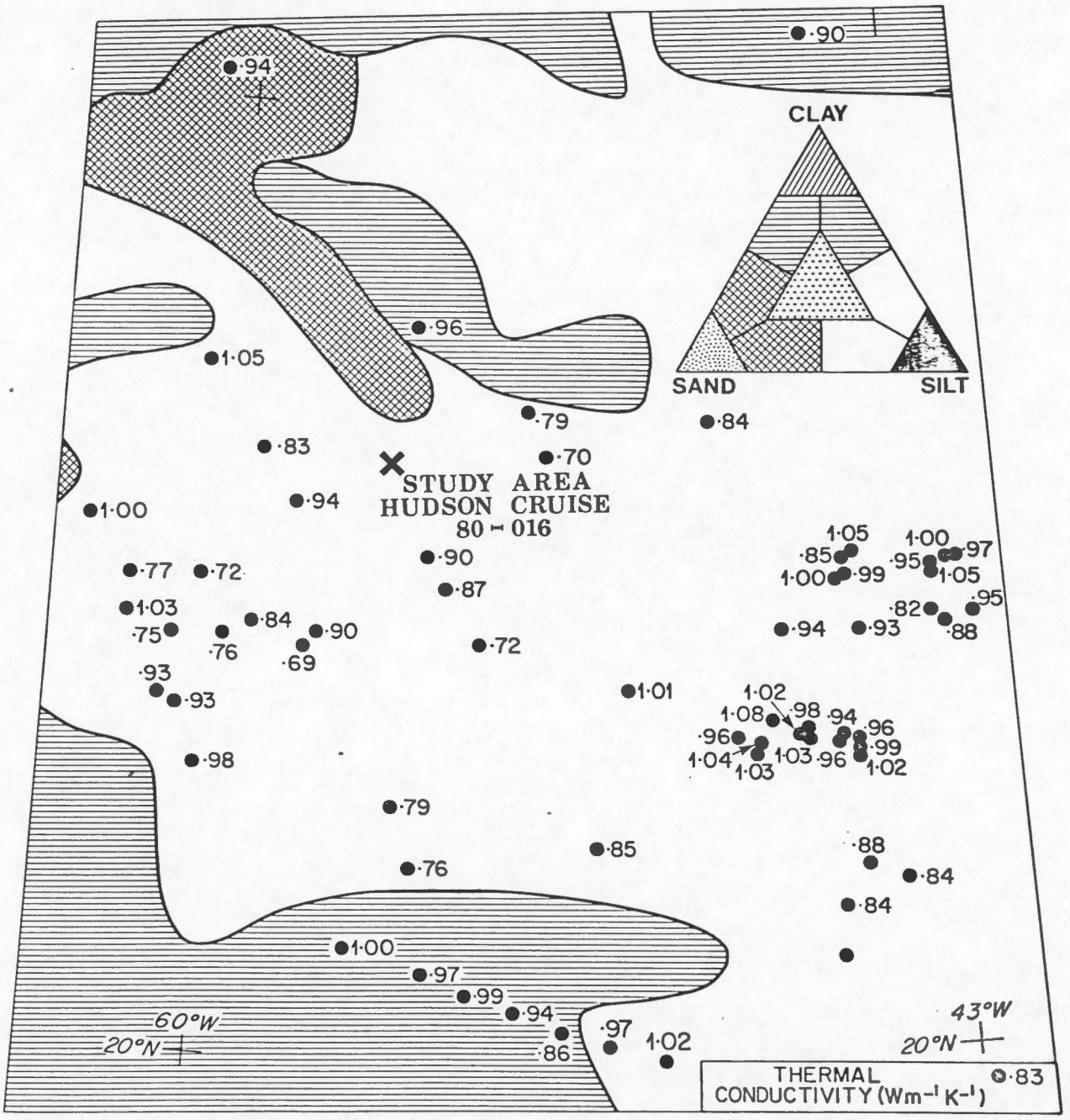

Fig. 6. Sediment thermal conductivities ($Wm^{-1}K^{-1}$) and surface sediment distribution.

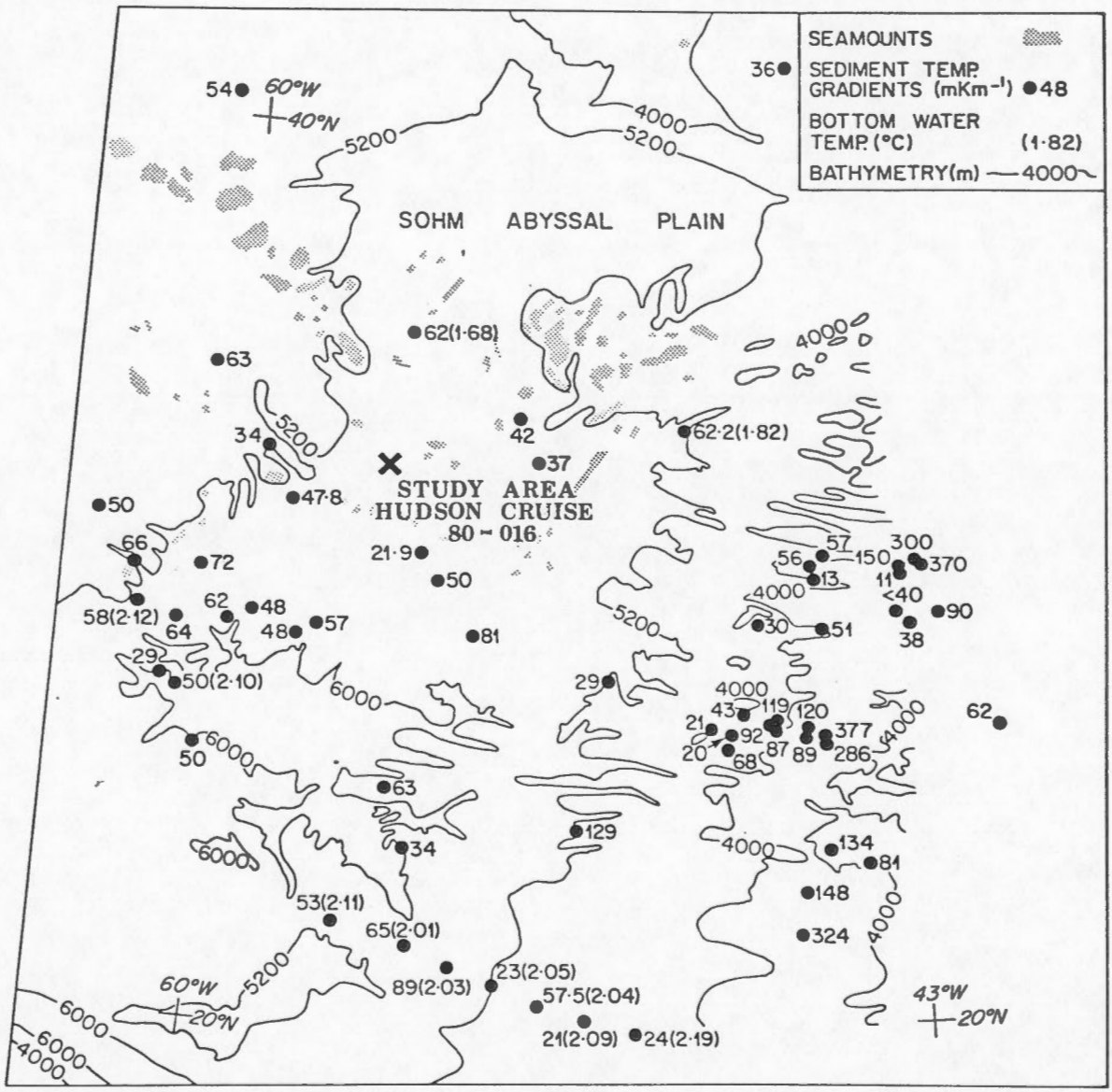

Fig. 7. Sediment temperature gradients (mKm^{-1}), bathymetry (m) and, in brackets, bottom water temperatures (°C).

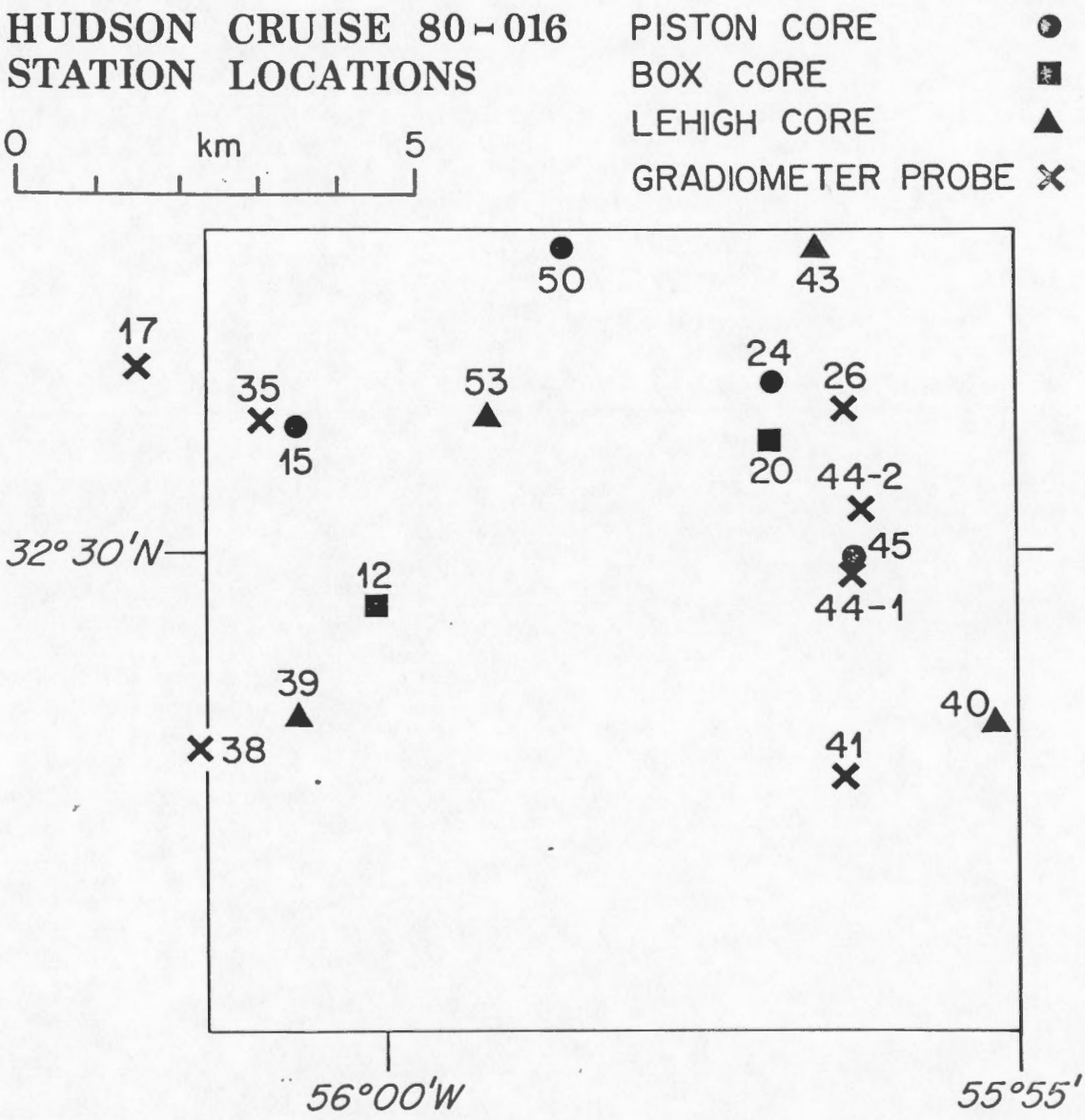

Fig. 8. Station locations, Hudson Cruise 80-016.

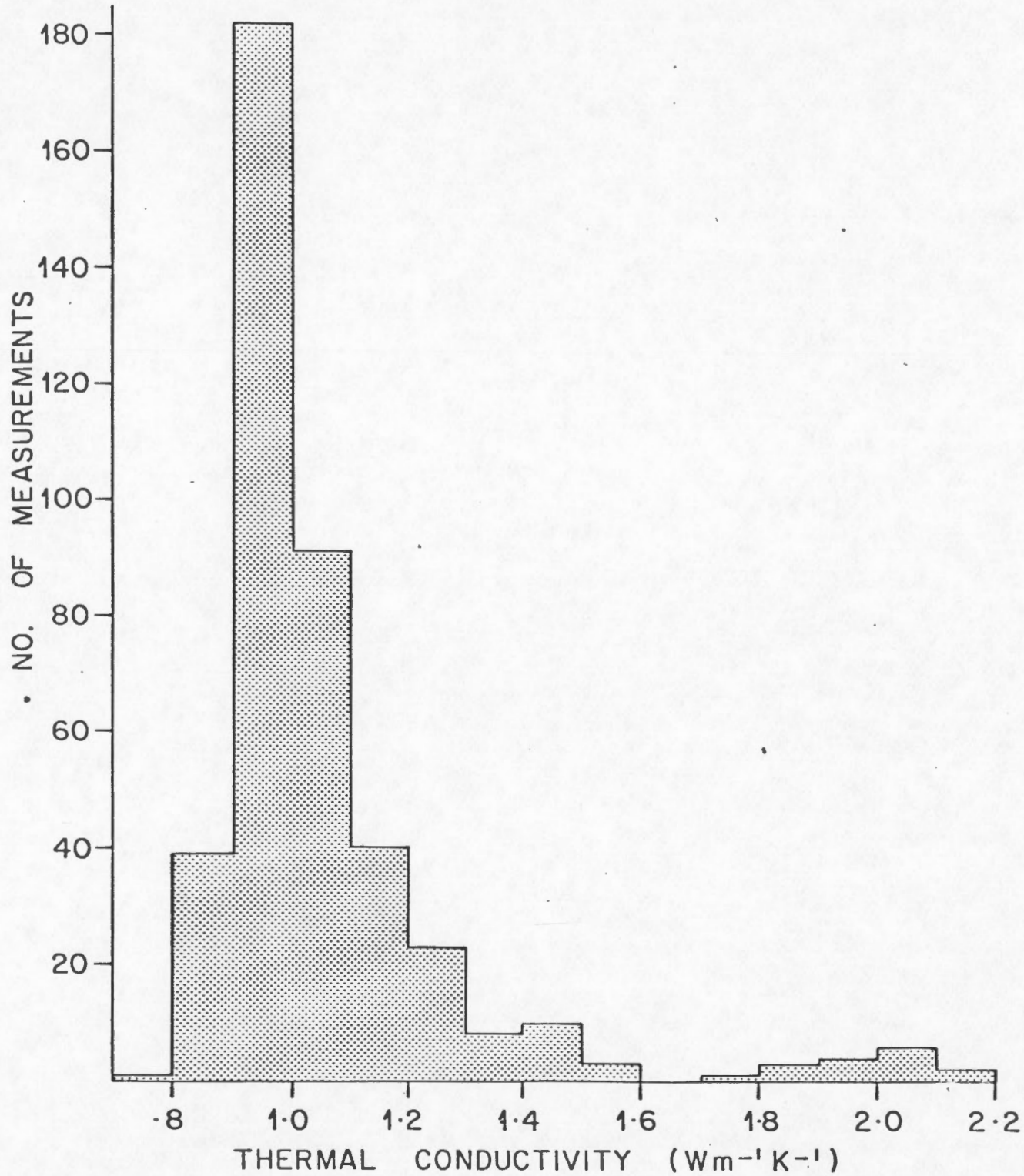

Fig. 9a. Histogram of thermal conductivity measurements, Hudson Cruise 80-016.

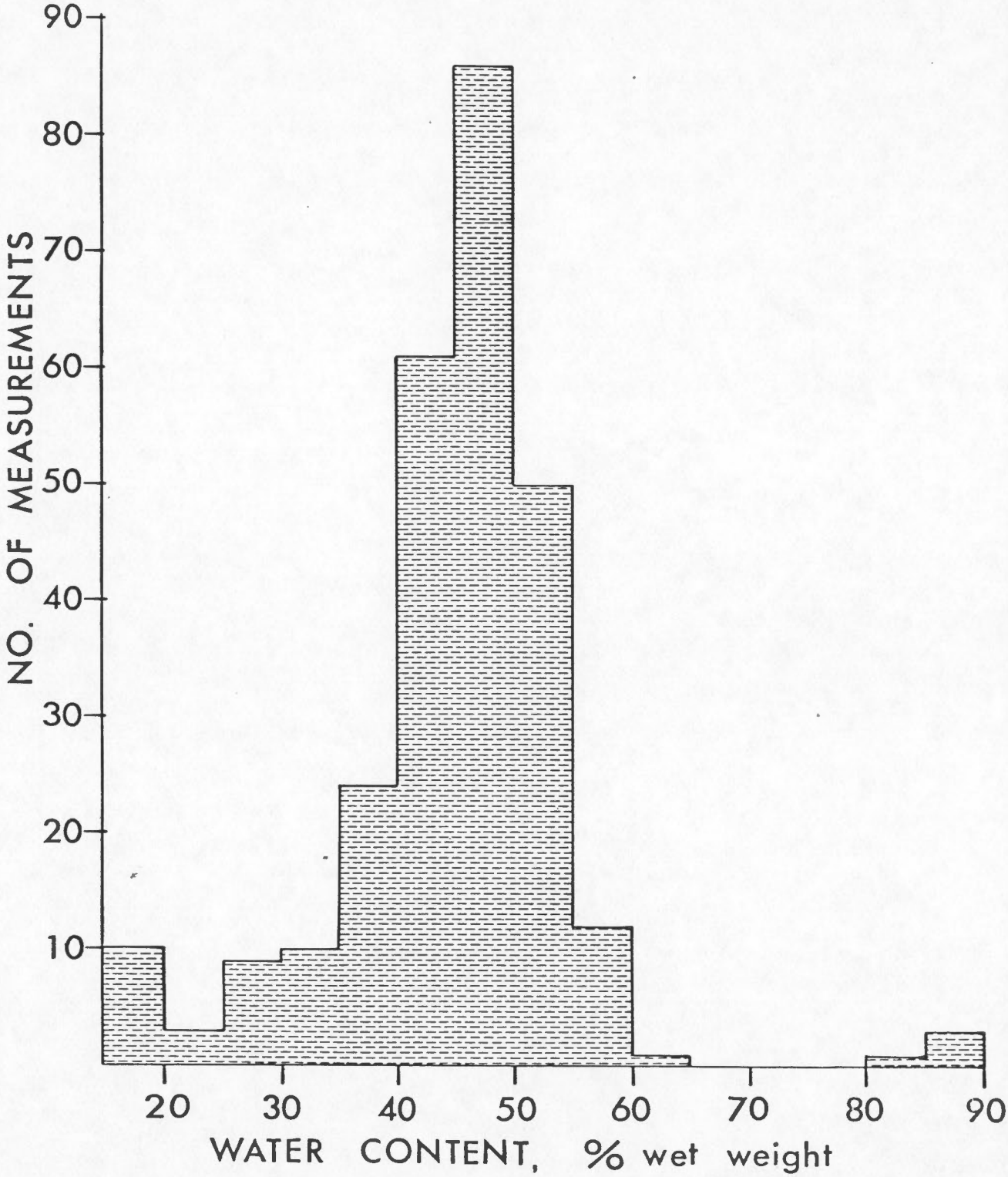

Fig. 9b. Histogram of sediment water content determinations, Hudson Cruise 80-016.

STATION 15. HUDSON 80-016. 32 30.85N 56 0.75W

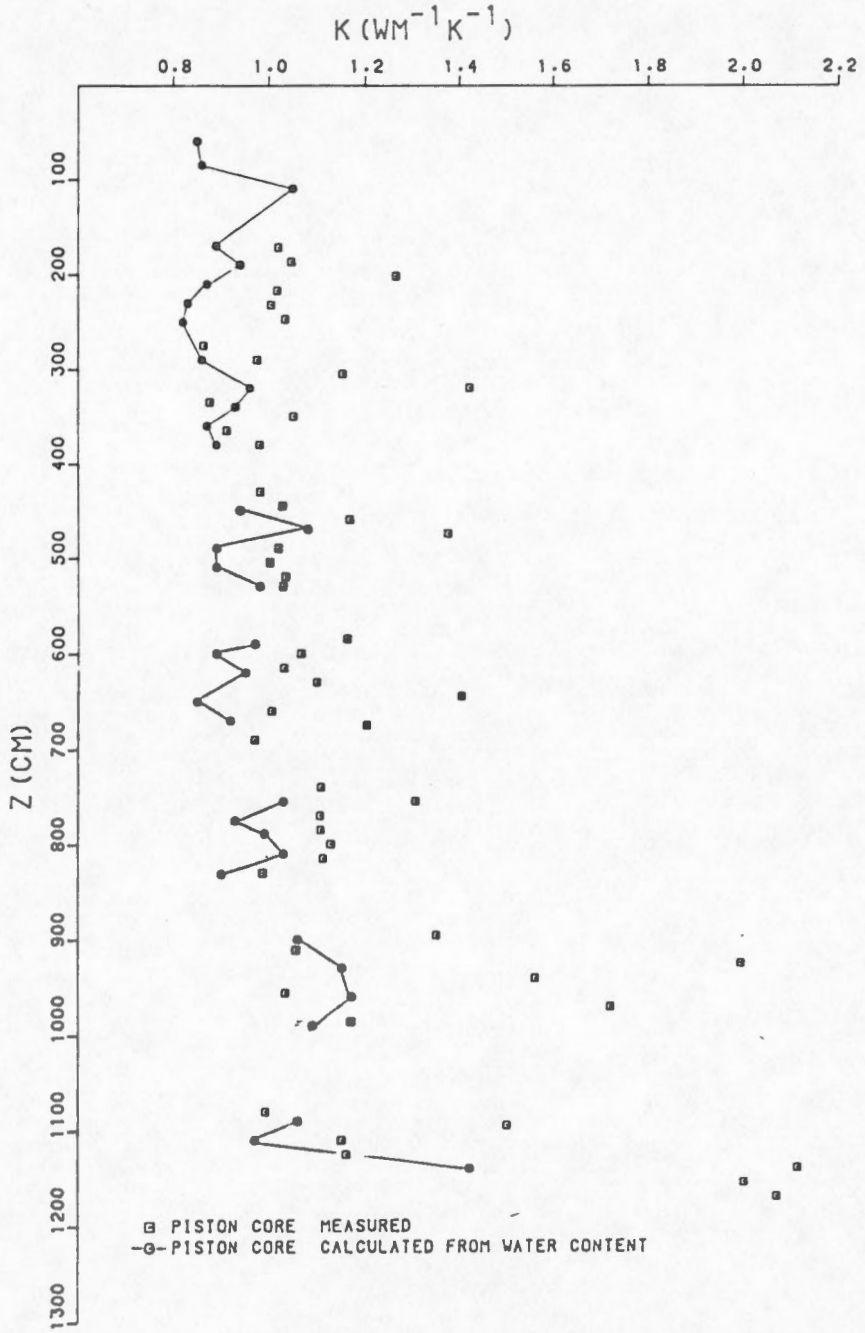

Fig. 10. Plot of measured and estimated (from water contents) thermal conductivities at station 15.

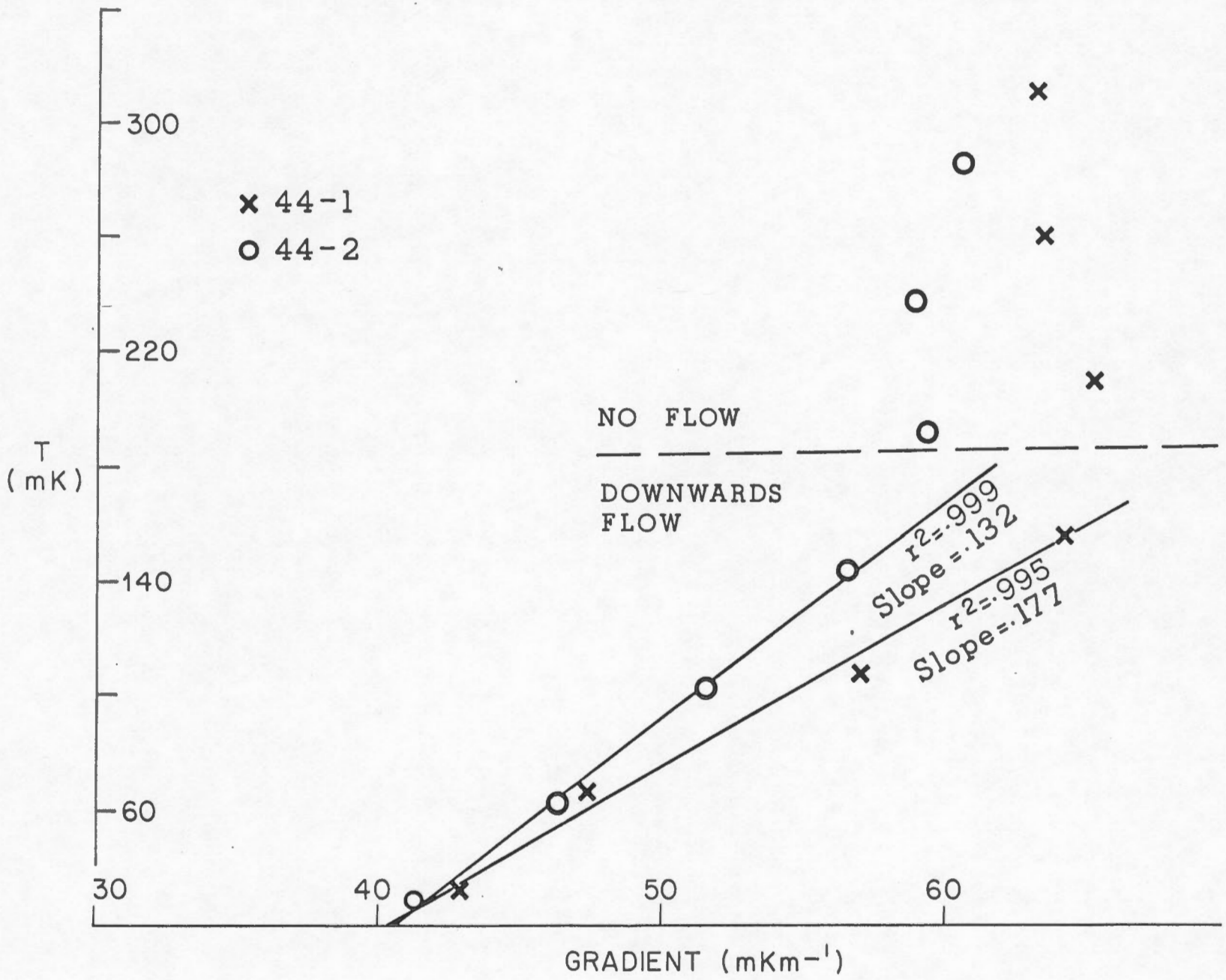

Fig. 11. Plot of temperature versus temperature gradient, station 44.

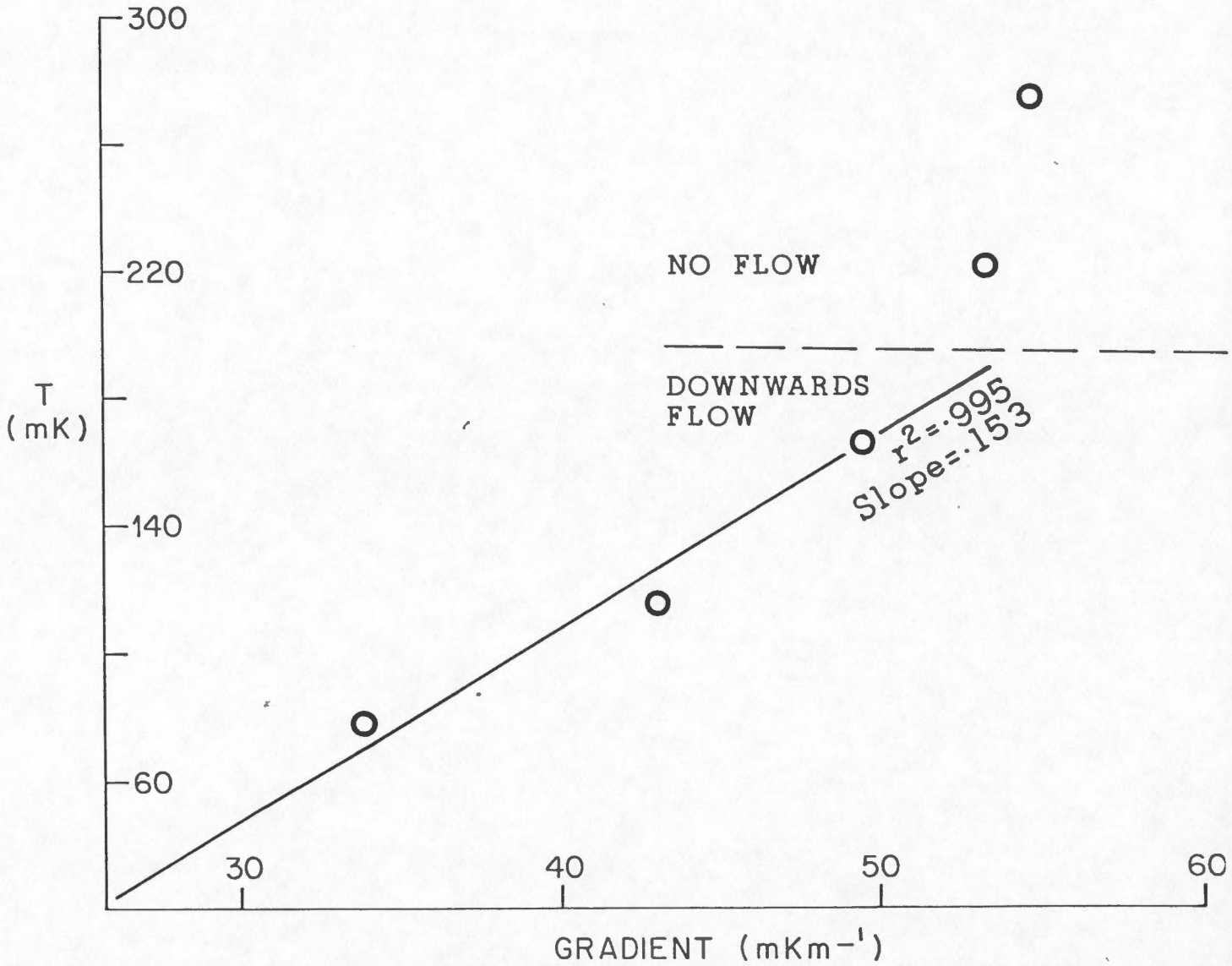

Fig. 12. Plot of temperature versus temperature gradient, 3 months after a 50 mK increase in bottom water temperature (sediment with an initial gradient of 55 mKm^{-1} and diffusivity of 2 x $10^{-7}m^2s^{-1}$), for depth interval from 1-5m with a 1m spacing.

APPENDIX A

TABLES OF HEAT FLOW DATA,

NORTHWESTERN ATLANTIC OCEAN,

SOHM ABYSSAL PLAIN AREA.

LEGEND

COLUMN	INFORMATION
1.	Latitude (N), degrees, minutes
2.	Longitude (W), degrees, minutes
3.	Water depth (m)
4.	Heat flow (mWm^{-2})
5.	Sediment temperature gradient (mKm^{-1})
6.	Number of sensors on probe
7.	Sensor spacing (m)
8.	Penetration of probe (m)
9.	Sediment thermal conductivity ($Wm^{-1}K^{-1}$)
10.	Type of thermal conductivity measurement W.C. - derived from water content N.P. - needle probe A - assumed from nearby measurement
11.	Bottom water temperature (°C)
12.	Bottom water temperature gradient (mKm^{-1})
13.	Reference number - see listing of references *not verified
14.	Comments

For references consulted, no corrections to heat flow values were applied.

LAT. N	LONG. W	Z_{H2O} (m)	H.F. (mWm^{-2})	T/ Z (mKm^{-1})	SENSORS #	SENSORS X(m)	SENSORS PEN(m)	CONDUCTIVITY ($Wm^{-1}K^{-1}$)	CONDUCTIVITY TYPE	BOTTOM WATER T(OC)	BOTTOM WATER T/ Z (mKm^{-1})	REF.	SEDIMENTS, COMMENTS
SOHM ABYSSAL PLAIN													
35.21	55.27	5469	60.7	62	3+			.96	N.P.	1.68	.18	8	1000m thick bottom layer
31.50	58.21	5614	44.8	47.8	3+			.94	N.P.			8	
32.42	52.35	5209	33.1	42				.79				3	
32.36	52.04	5161	25.5	37				.70				3	
SOHM ABYSSAL PLAIN/ABYSSAL HILLS													
30.27	55.02	5594	19.7	21.9	3+			.90	N.P.		<.01	8	400m bottom sed. layer
29.51	54.36	5610	43.5	50				.87	W.C.			11	
ABYSSAL HILLS													
29.00	59.11	5811	39.8	48	2	2		.84	W.C.			2	
25.18	55.44	5932	49.8	63	2	2		.79	W.C.			2	
24.04	55.15	5984	25.5	34	2	2		.76	W.C.			2	
28.30	57.59	5800	33.1	48	2	2		.69	W.C.			2	
29.56	60.33	5715	55.3	72	2	2		.72	W.C.			2	
21.00	52.56	4680	21.4	23	3		2.5	.94	N.P.	2.05		6	
21.19	53.58	5300	88.4	89	5		7.2	.99	N.P.	2.03		6	
21.44	55.00	5300	63.2	65	5		7.1	.97	N.P.	2.01		6	
22.14	56.39	5980	53.6	53	5		9.0	1.00	N.P.	2.11		6	
25.58	60.19	5874	49.4	50	4		9	.98				9	
27.26	61.18	5770	26.8	29	3		12	.93				9	
28.38	59.43	5324	47.3	62	3		10	.76				10	
28.43	57.33	5902	51.5	57	2		12	.90				10	
28.41	53.41	5299	58.2	81	3		7	.72				10	
24.24	51.02	5417	110	129	4		8	.85				10	
27.15	60.37	5640	46.9	50	5		8.7	.93	N.P.	2.10		6	
ABYSSAL HILLS/BERMUDA RISE													
29.47	62.12	4865	50.2	66	2	2		.77	W.C.			2	
27.15	60.37	5640	46.9	50	5		8.7	.93	N.P.	2.10		6	
28.44	61.03	5813	48.2	64	3		11	.75				10	

LAT. N	LONG. W	Z_{H2O} (m)	H.F. (mWm^{-2})	T/ Z (mKm^{-1})	SENSORS #	SENSORS X(m)	SENSORS PEN(m)	CONDUCTIVITY ($Wm^{-1}K^{-1}$)	CONDUCTIVITY TYPE	BOTTOM WATER T(OC)	BOTTOM WATER T/ Z (mKm^{-1})	REF.	SEDIMENTS, COMMENTS
BERMUDA RISE/SOHM ABYSSAL PLAIN													
32.37	59.10	4907	28.5	34				.83				3	
ABYSSAL HILLS/MID ATLANTIC RIDGE													
27.40	50.15	4774	29.3	29	3		7	1.01				10	
MID ATLANTIC RIDGE													
33.18	48.16	4629	51.9	62.2	3+			.84	A	1.82	.3	8	water temperature profile
28.56	46.44	4370	28.1	30				.94	W.C.			11	
28.47	44.55	3940	47.3	51				.93	W.C.			11	
29.04	43.12	3080	33.5	40				.82	W.C.			11	
28.51	42.49	3520	33.9	38				.88	W.C.			11	
23.06	45.39	3983	125.6	148	2			.84	N.P.			12	
23.34	44.14	4960	67.0	81	2			.84	N.P.			12	sedimentation rate: .5cm/1000yr
23.57	44.59	3493	117.2	134				.88	N.P.			12	partial probe penetration
21.56	45.46	3372	272.2	324	2			.84	N.P.			12	
20.01	49.46	4650	24.3	24	5		5	1.02	N.P.	2.19		6	
20.21	50.52	4820	20.5	21	4		6.9	.97	N.P.	2.09		6	
20.39	51.56	5300	52.3	61	3		2.5	.86	A	2.04		6	
20.39	51.56	5300	46.1	54	3		2.3	.86	A	2.04		6	
29.54	45.07	3244	12.6	13				.99				3	
30.21	44.54	3889	59.9	57				1.05				3	
30.13	45.06	3853	47.3	56				.85				3	
26.21	40.56	4695	60.7	62				.98				3	
28.515	42.11	3580	85.4	90	2		0.7	.95				7*	
30.03.8	42.27.3	4900	360	370	3		1.3	.97				7*	
29.57.8	42.59.9	3050	142	150	2		1.4	.95				7*	
29.53.8	42.59.9	2880	11.5	11	4		1.3	1.05				7*	
30 6.0	42.36.5	2960	300	300	2		1.0	1.00				7*	
26.55	47.00	4390	46.9	43	1		2	1.08				10	
26.15	47.22	3890	69.5	68	3		4	1.03				10	
26.28	47.15	4565	20.9	20	2		3	1.04				10	
26.35	46.16	3984	89.6	87	4		5	1.03				10	

LAT. N	LONG. W	Z_{H2O} (m)	H.F. (mWm^{-2})	T/ Z (mKm^{-1})	SENSORS #	SENSORS X(m)	SENSORS PEN(m)	CONDUCTIVITY ($Wm^{-1}K^{-1}$)	CONDUCTIVITY TYPE	BOTTOM WATER T(OC)	BOTTOM WATER T/ Z (mKm^{-1})	REF.	SEDIMENTS, COMMENTS
MID ATLANTIC RIDGE (CONT'D.)													
26.44	46.10	3607	116	119	2		2	.98				10	
26.35	46.15	3962	93.8	92	3		3	1.02				10	
26.29	45.23	3594	113	120	2		3	.94				10	
26.24	45.27	3618	85.4	89	1		2	.96				10	
26.22	45.01	3102	360	377	2		3	.96				10	
25.13	45.02	2497	283	286	2		2	.99				10	
25.16	45.01	2568	136	134	3		5	1.02				10	
CONTINENTAL RISE													
40.33	60.49	4981	50.7	54	4		11	.94				9	
41.31	45.08	4845	32.2	36	3		12	.90				9	
34.25	60.40	4766	66.2	63	3		13	1.05				9	
29.06	62.00	5260	59.0	58	5		8.6	1.03	N.P.	2.12		6	
30.54	63.23	5030	49.8	50	4		8.6	1.00	N.P.			6	
25.29	64.34	5680	45.6	56.9				.80	W.C.			13	
25.26.5	66.40	5580	51.1	63.8				.80	W.C.			13	
27.05	67.56	5200	44.8	57.2				.79	W.C.			13	
28.44	69.05	5330	49.4	58.2				.86	W.C.			13	
28.51	66.50	5240	49.8	61.6				.81	W.C.			13	
28.54	64.39	4900	46.5	61.3				.76	W.C.			13	
30.27	67.58	5230	44.0	55.1				.80	W.C.			13	
NARES ABYSSAL PLAIN													
23.14	66.36	5605	56.9	61	2		9.5	.93	W.C.	207		5	water temperature profile
23.37	67.54	5650	44.4	52.9				.84	W.C.	2.2		13	
21.47	68.51	5560	53.2	61.2				.88	W.C.	2.2		13	
21.54	66.37	5640	49.8	60.9				.81	W.C.	2.2		13	
23.40	65.37	5800	47.3	59.0				.81	W.C.	2.2		13	
-	-	-	63 (mean)	-								4	5 lines of closely spaced measurements in 1978; range in heat flow 40-764

LAT. N	LONG. W	Z_{H2O} (m)	H.F. (mWm^{-2})	T/ Z (mKm^{-1})	SENSORS #	SENSORS X(m)	SENSORS PEN(m)	CONDUCTIVITY ($Wm^{-1}K^{-1}$)	CONDUCTIVITY TYPE	BOTTOM WATER T(OC)	BOTTOM WATER T/ Z (mKm^{-1})	REF.	SEDIMENTS, COMMENTS
HATTERAS ABYSSAL PLAIN													
23.20	70.02.5	5480	46.9	53.5	2			.88	W.C.	2.2		13	
23.28	72.18.5	5300	49.0	65.9	2			.74	W.C.	2.2		13	
25.13.5	73.16	5310	45.2	52.9	2			.85	W.C.	2.2		13	
26.59	72.13	5150	45.6	58.4	2			.78	W.C.	2.2		13	
25.18	69.01	5580	49.0	55.3	2			.88	W.C.	2.2		13	
NEW ENGLAND SEAMOUNTS													
39.32	65.49.5	4330	45.2	47.3	2	2		.26	W.C.			1	
39.33	66.17	4325	62.4	56.8	2	2		.99	W.C.			1	
39.47	65.15.5	4467	42.7	47.7	2	2		.90	W.C.			1	
39.26.5	65.09	4757	46.9	53.3	2	2		.88	W.C.			1	
39.46	66.28	3922	47.7	53.9	2	2		.88	W.C.			1	

APPENDIX B

THERMAL CONDUCTIVITIES,

HUDSON CRUISE 80-016,

SOHM ABYSSAL PLAIN

SEDIMENT THERMAL CONDUCTIVITY
HUDSON CRUISE 80-016, SOHM ABYSSAL PLAIN

BOX CORES, HUDSON 80-016
STATION 12, 32 29.63N 56 0.10W

DEPTH(CM)	THERMAL CONDUCTIVITY($WM^{-1}K^{-1}$)	THERMAL RESISTANCE(M^2K/W)
3	.81	.04
12	.90	.14
21	.97	.23
30	1.19	.31
39	1.18	.38

MEAN CONDUCTIVITY - 1.01
HARMONIC MEAN CONDUCTIVITY - 1.02

SEDIMENT THERMAL CONDUCTIVITY
HUDSON CRUISE 80-016, SOHM ABYSSAL PLAIN

BOX CORES, HUDSON 80-016
STATION 20, 32 30.77N 55 56.96W

DEPTH(CM)	THERMAL CONDUCTIVITY($WM^{-1}K^{-1}$)	THERMAL RESISTANCE(M^2K/W)
5	.87	.06
17	1.09	.17
29	1.15	.27
41	1.02	.39
53	1.04	.51

MEAN CONDUCTIVITY - 1.03
HARMONIC MEAN CONDUCTIVITY - 1.05

STATION 15, HUDSON 80-016, 32 30.85N 56 0.75W
PISTON CORE

DEPTH(CM)	THERMAL CONDUCTIVITY($W m^{-1} K^{-1}$)	THERMAL RESISTANCE($m^2 K/W$)
172	1.02	1.69
187	1.05	1.83
202	1.26	1.95
217	1.02	2.10
232	1.00	2.25
247	1.03	2.39
275	.86	2.71
290	.98	2.87
305	1.15	3.00
320	1.42	3.10
335	.88	3.28
350	1.05	3.42
365	.91	3.58
380	.98	3.74
430	.98	4.25
445	1.03	4.39
460	1.17	4.52
475	1.37	4.63
490	1.02	4.78
505	1.00	4.93
520	1.03	5.07
530	1.03	5.17
585	1.16	5.64
600	1.07	5.78
615	1.03	5.93
630	1.10	6.06
645	1.40	6.17
660	1.01	6.32
675	1.20	6.45
690	.97	6.60
740	1.11	7.05
755	1.30	7.17
770	1.11	7.30
785	1.11	7.44
800	1.13	7.57
815	1.11	7.71
830	.99	7.86
896	1.35	8.35
911	1.06	8.49
926	1.99	8.56
941	1.56	8.66
956	1.03	8.81
971	1.72	8.89
986	1.17	9.02
1080	.99	9.97
1095	1.50	10.07
1110	1.15	10.20
1125	1.16	10.33
1140	2.11	10.40
1155	2.00	10.47
1170	2.07	10.55

MEAN CONDUCTIVITY - 1.19
HARMONIC MEAN CONDUCTIVITY - 1.11
SEDIMENT THERMAL CONDUCTIVITY
HUDSON CRUISE 80-016, SOHM ABYSSAL PLAIN

STATION 15, HUDSON 80-016, 32 30.85N 56 0.75W
GRAVITY CORE

DEPTH(CM)	THERMAL CONDUCTIVITY($W M^{-1} K^{-1}$)	THERMAL RESISTANCE($M^2 K/W$)
15	.87	.17
30	.84	.35
45	1.00	.50
60	.97	.66
75	1.03	.80
90	1.10	.94
105	1.18	1.07
120	.96	1.22
135	1.18	1.35
150	1.06	1.49

MEAN CONDUCTIVITY - 1.02
HARMONIC MEAN CONDUCTIVITY - 1.01

STATION 24, HUDSON 80-016, 32 31.1N 55 56.92W
GRAVITY CORE

DEPTH(CM)	THERMAL CONDUCTIVITY($W M^{-1} K^{-1}$)	THERMAL RESISTANCE($M^2 K/W$)
5	.84	.06
20	.92	.22
35	.82	.41
50	1.03	.55
65	.96	.71
80	.91	.87
95	.96	1.03
110	.95	1.19
125	1.06	1.33
137	1.05	1.45
150	.95	1.58
165	.92	1.75
172	1.05	1.82
180	1.48	1.87
190	.98	1.97

MEAN CONDUCTIVITY - .99
HARMONIC MEAN CONDUCTIVITY - .96

STATION 24, HUDSON 80-016, 32 31.1N 55 56.92W
PISTON CORE

DEPTH(CM)	THERMAL CONDUCTIVITY($W M^{-1} K^{-1}$)	THERMAL RESISTANCE($M^2 K/W$)
65	.86	.76
80	1.02	.90
140	.90	1.57
155	.94	1.73
190	.93	2.11
205	.95	2.27
220	.96	2.42
290	1.03	3.11
305	1.04	3.25
320	.96	3.41
335	1.03	3.55
350	1.02	3.70
365	1.03	3.85
380	1.02	3.99
395	.96	4.15
410	1.01	4.30
425	.97	4.45
500	1.07	5.15
515	1.30	5.27
530	.96	5.42
545	.93	5.58
560	.93	5.75
575	1.02	5.89
590	1.02	6.04
605	.96	6.20
675	1.00	6.89
690	1.49	6.99
800	.88	8.24
815	1.04	8.39
830	1.34	8.50
845	1.10	8.64
860	1.04	8.78
875	1.13	8.91
960	1.21	9.61
975	1.91	9.69
990	1.91	9.77
1055	1.80	10.13
1070	2.03	10.21
1085	2.12	10.28

MEAN CONDUCTIVITY - 1.15
HARMONIC MEAN CONDUCTIVITY - 1.06

STATION 39, HUDSON 80-016, 32 28.8N 56 0.74W
LEHIGH CORE

DEPTH(CM)	THERMAL CONDUCTIVITY($WM^{-1}K^{-1}$)	THERMAL RESISTANCE(M^2K/W)
55	.99	.55
70	1.00	.70
85	1.21	.83
100	1.10	.96
115	1.22	1.09
130	1.04	1.23
145	1.02	1.38
160	1.07	1.52
175	1.03	1.66
190	1.04	1.81
205	.96	1.96
220	1.07	2.11
235	1.06	2.25
250	.97	2.40
265	.96	2.56
280	1.00	2.71
295	1.02	2.86
310	1.28	2.97

MEAN CONDUCTIVITY - 1.06
HARMONIC MEAN CONDUCTIVITY - 1.04

STATION 40, HUDSON 80-016, 32 28.83N 55 55.21W
LEHIGH CORE

DEPTH(CM)	THERMAL CONDUCTIVITY($WM^{-1}K^{-1}$)	THERMAL RESISTANCE(M^2K/W)
5	.98	.05
10	1.31	.09
25	.95	.25
40	.97	.40
50	1.04	.50

MEAN CONDUCTIVITY - 1.05
HARMONIC MEAN CONDUCTIVITY - 1.01

STATION 45, HUDSON 80-016, 32 29.96N 55 56.29W
GRAVITY CORE

DEPTH(CM)	THERMAL CONDUCTIVITY($W M^{-1} K^{-1}$)	THERMAL RESISTANCE($M^2 K/W$)
5	.84	.06
20	.86	.23
35	.97	.39
50	1.03	.53
65	.90	.70
80	.96	.86
95	.93	1.02
110	1.12	1.15

MEAN CONDUCTIVITY - .95
HARMONIC MEAN CONDUCTIVITY - .95

STATION 50, HUDSON 80-016, 32 32.05N, 55 58.61W
GRAVITY CORE

DEPTH(CM)	THERMAL CONDUCTIVITY($W M^{-1} K^{-1}$)	THERMAL RESISTANCE($M^2 K/W$)
10	.86	.12
25	.93	.28
40	.88	.45
55	.91	.61
70	.89	.78
85	.92	.94
100	.91	1.11
115	.89	1.28
130	.90	1.45
145	.91	1.61
160	.93	1.77
175	.94	1.93

MEAN CONDUCTIVITY - .90
HARMONIC MEAN CONDUCTIVITY - .90

STATION 45, HUDSON 80-016, 32 29.96N 55 56.29W
PISTON CORE

DEPTH(CM)	THERMAL CONDUCTIVITY($WM^{-1}K^{-1}$)	THERMAL RESISTANCE(M^2K/W)
10	.95	.11
20	.90	.22
30	1.11	.31
40	.99	.41
90	1.17	.84
105	.91	1.00
120	.95	1.16
135	.93	1.32
150	1.47	1.42
165	.97	1.58
180	.86	1.75
195	.90	1.92
223	.95	2.21
238	.95	2.37
253	.95	2.53
268	.92	2.69
283	.91	2.86
298	1.07	3.00
313	.94	3.16
328	.92	3.32
343	.94	4.01
408	1.11	4.15
423	.97	4.30
438	.97	4.46
453	.95	4.61
468	.94	4.77
483	1.02	4.92
498	1.03	5.07
513	.99	5.22
568	1.11	5.71
583	1.02	5.86
598	.97	6.02
613	.96	6.17
628	.96	6.33
643	1.00	6.48
658	1.02	6.63
673	.95	6.78
688	1.04	6.93
723	.98	7.29
753	.98	7.59
768	1.09	7.73
783	1.13	7.86
798	1.02	8.01
813	1.03	8.16
828	.99	8.31
843	1.09	8.45
873	1.00	8.75
888	1.08	8.88
903	1.07	9.02
918	1.01	9.17
933	1.05	9.32
948	.97	9.47
963	1.00	9.62
978	1.01	9.77
993	1.13	9.90
1018	1.24	10.10
1033	1.22	10.23
1048	1.20	10.35
1063	1.11	10.49
1078	1.13	10.62
1093	1.12	10.75
1108	1.24	10.87
1123	1.15	11.00
1178	1.41	11.39
1193	1.11	11.53
1208	1.84	11.61
1223	1.84	11.69
1238	2.00	11.77
1253	2.02	11.84
1268	1.93	11.92
1278	2.08	11.97

MEAN CONDUCTIVITY - 1.11
HARMONIC MEAN CONDUCTIVITY - 1.07

STATION 50, HUDSON 80-016, 32 32.05N, 55 58.61W
PISTON CORE

DEPTH(CM)	THERMAL CONDUCTIVITY($WM^{-1}K^{-1}$)	THERMAL RESISTANCE(M^2K/W)
62	.74	.84
67	.83	.90
72	.85	.96
77	.94	1.02
82	.88	1.07
87	.84	1.13
92	.88	1.19
97	.87	1.25
102	.90	1.30
107	.85	1.36
112	.97	1.41
117	.93	1.47
122	.95	1.52
127	.96	1.57
132	.93	1.63
137	.91	1.68
147	.87	1.80
154	.84	1.88
161	1.47	1.93
169	.94	2.01
176	.94	2.09
184	1.03	2.16
191	.96	2.24
199	.87	2.33
206	.88	2.41
214	.90	2.50
229	.86	2.67
244	.87	2.84
251	.90	2.92
259	.89	3.01
266	.97	3.09
274	.92	3.17
281	1.57	3.22
289	.92	3.30
296	.93	3.38
313	.89	3.57
321	.89	3.65
328	.91	3.73
336	1.01	3.81
343	1.19	3.87
351	.93	3.95
358	.91	4.03
366	.93	4.11
373	1.24	4.17
381	1.04	4.25
388	.96	4.33
396	.93	4.41
403	.99	4.48
411	.93	4.56
426	.93	4.72
433	.98	4.80
441	.95	4.88

458	.93	5.06
465	.97	5.14
473	1.09	5.20
480	.91	5.29
488	.91	5.37
495	.95	5.45
503	.96	5.53
510	.93	5.61
518	1.04	5.68
525	.91	5.76
533	.91	5.84
540	.93	5.93
548	.98	6.00
555	1.06	6.07
563	.96	6.15
570	.88	6.24
578	.93	6.32
585	.93	6.40
593	.96	6.48
600	.99	6.55
613	.99	6.68
620	.92	6.76
628	1.02	6.83
635	.94	6.91
643	.96	6.99
650	1.01	7.06
658	1.41	7.12
665	.92	7.20
673	.95	7.28
680	1.24	7.34
688	.94	7.42
703	.95	7.58
710	1.14	7.64
718	.97	7.72
725	.96	7.80
733	.95	7.88
740	.97	7.96
748	1.06	8.03
755	.90	8.11
765	1.04	8.20
772	1.26	8.26
780	1.25	8.32
787	.99	8.40
795	.95	8.48
802	.94	8.56
810	.98	8.63
817	.92	8.71
825	.93	8.79
832	.95	8.87
840	.98	8.95
847	1.24	9.01
855	.99	9.09
862	.93	9.17
870	1.03	9.24
877	.94	9.32
885	1.09	9.39
892	.91	9.47
900	.95	9.55
907	.98	9.63
920	1.02	9.75
927	1.20	9.81
935	.91	9.89
942	.94	9.97
950	.93	10.06
957	.94	10.13

972	1.11	10.28
980	.94	10.36
987	.97	10.43
995	.95	10.51
1003	1.31	10.57
1010	.97	10.65
1018	.97	10.73
1025	1.00	10.80
1033	.96	10.88
1040	.94	10.96
1048	1.00	11.04
1055	1.04	11.10
1063	.95	11.19
1070	.96	11.26
1078	.98	11.34
1085	.85	11.43
1093	.87	11.52
1100	.85	11.60
1108	1.10	11.67
1115	1.09	11.74
1123	1.25	11.80
1130	1.20	11.86
1138	1.25	11.92
1145	1.27	11.98
1153	1.45	12.03
1160	1.28	12.09
1168	1.29	12.15
1175	1.42	12.20
1183	1.30	12.26
695	.94	7.05

MEAN CONDUCTIVITY - 1.00
HARMONIC MEAN CONDUCTIVITY - .99

STATION 53 32 30.91N 55 59.19W
LEHIGH CORE

DEPTH(CM)	THERMAL CONDUCTIVITY($W m^{-1} K^{-1}$)	THERMAL RESISTANCE($m^2 K/W$)
44	.91	.48
59	.94	.64
74	.96	.80
89	.94	.96
99	.92	1.07
110	1.00	1.18
125	.93	1.34
140	.94	1.50
150	.96	1.60
160	.90	1.71
175	1.09	1.85
190	.90	2.02
205	.88	2.19
220	1.12	2.32
235	.92	2.49
260	1.15	2.70
275	.92	2.87
290	1.29	2.98
305	.94	3.14
320	.91	3.31
335	.91	3.47
350	1.09	3.61
365	.96	3.76
380	1.02	3.91
395	.88	4.08
410	1.19	4.21
420	.98	4.31

MEAN CONDUCTIVITY - .98
HARMONIC MEAN CONDUCTIVITY - .97

BOX CORES. HUDSON 80-016

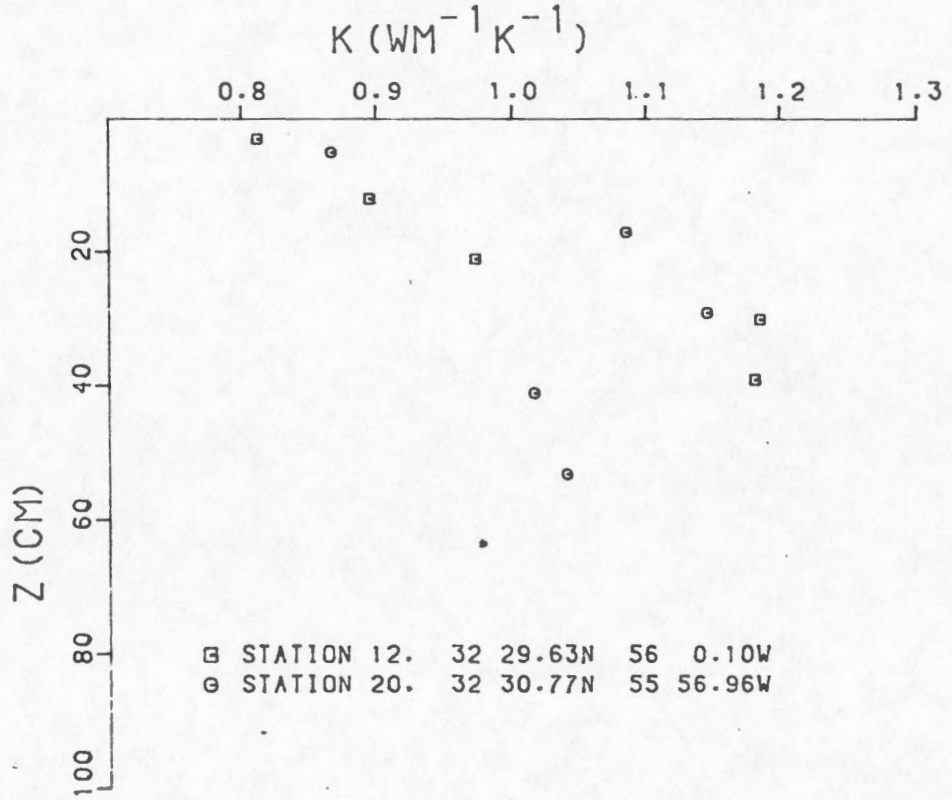

STATION 15. HUDSON 80-016. 32 30.85N 56 0.75W

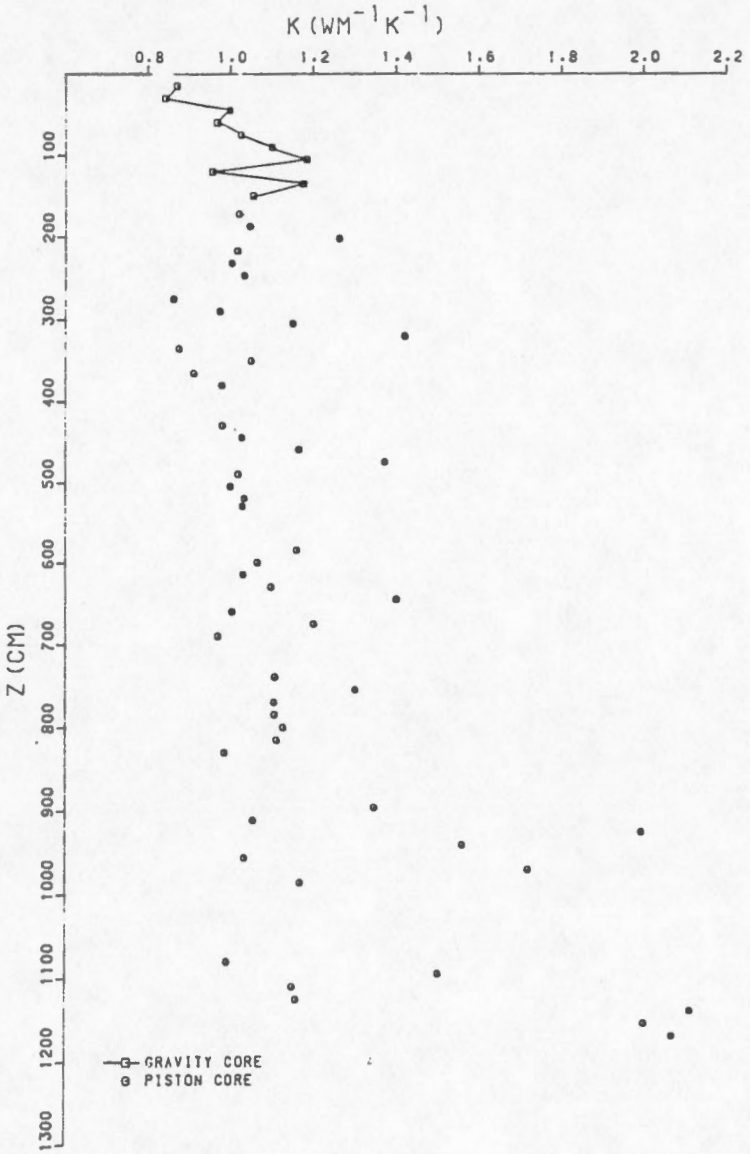

STATION 24. HUDSON 80-016. 32 31.1N 55 56.92W

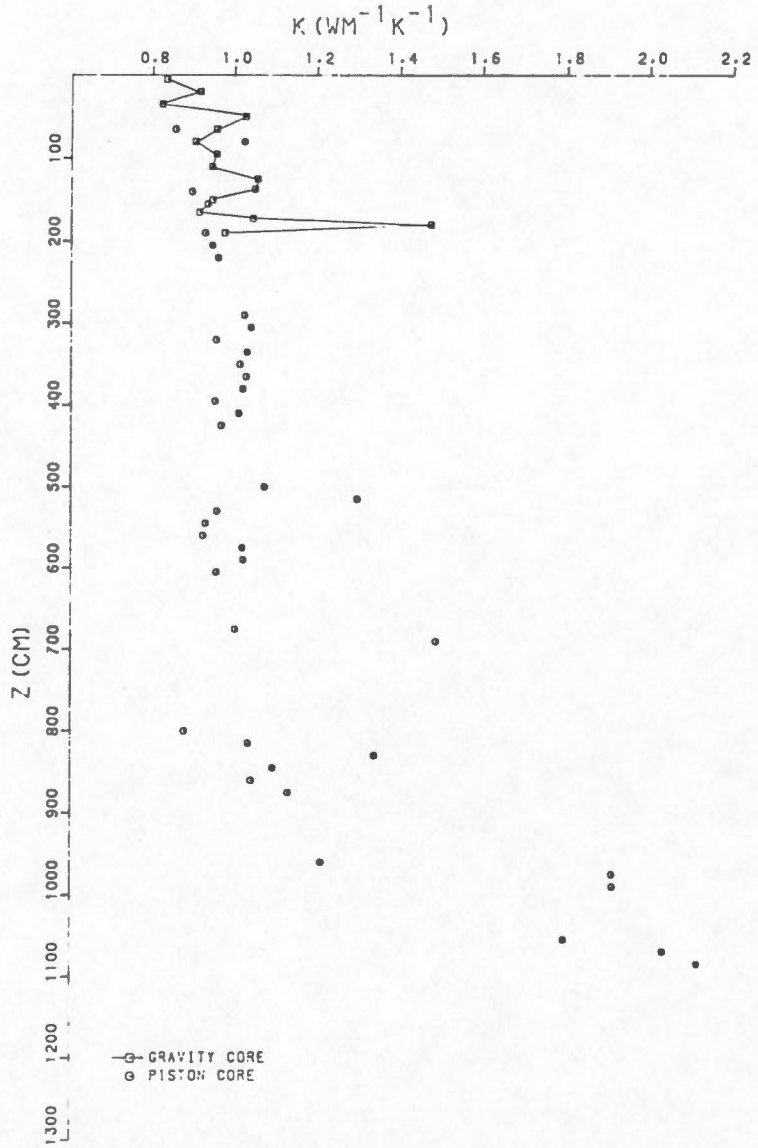

STATION 39. HUDSON 80-016. 32 28.8N 56 0.74W

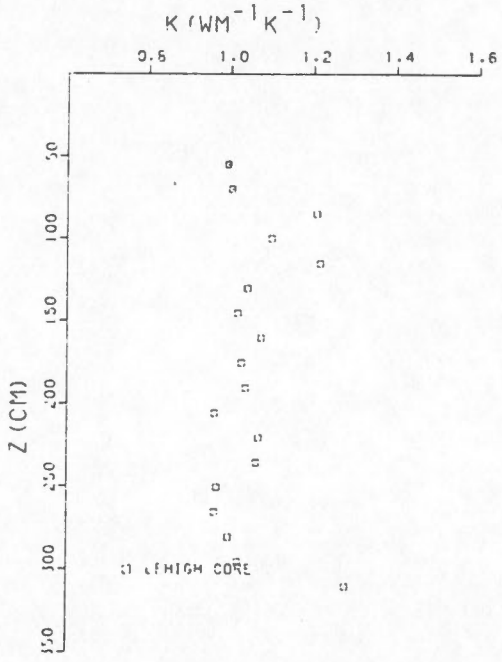

STATION 40. HUDSON 80-016. 32 28.83N 55 55.21W

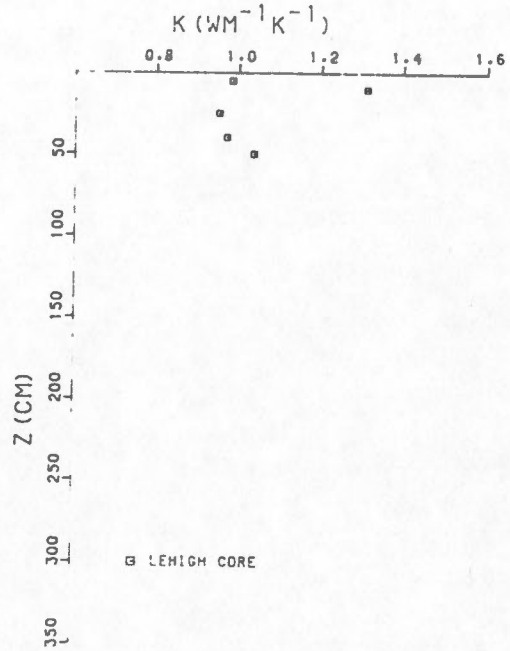

STATION 45. HUDSON 80-016. 32 29.96N 55 56.29W

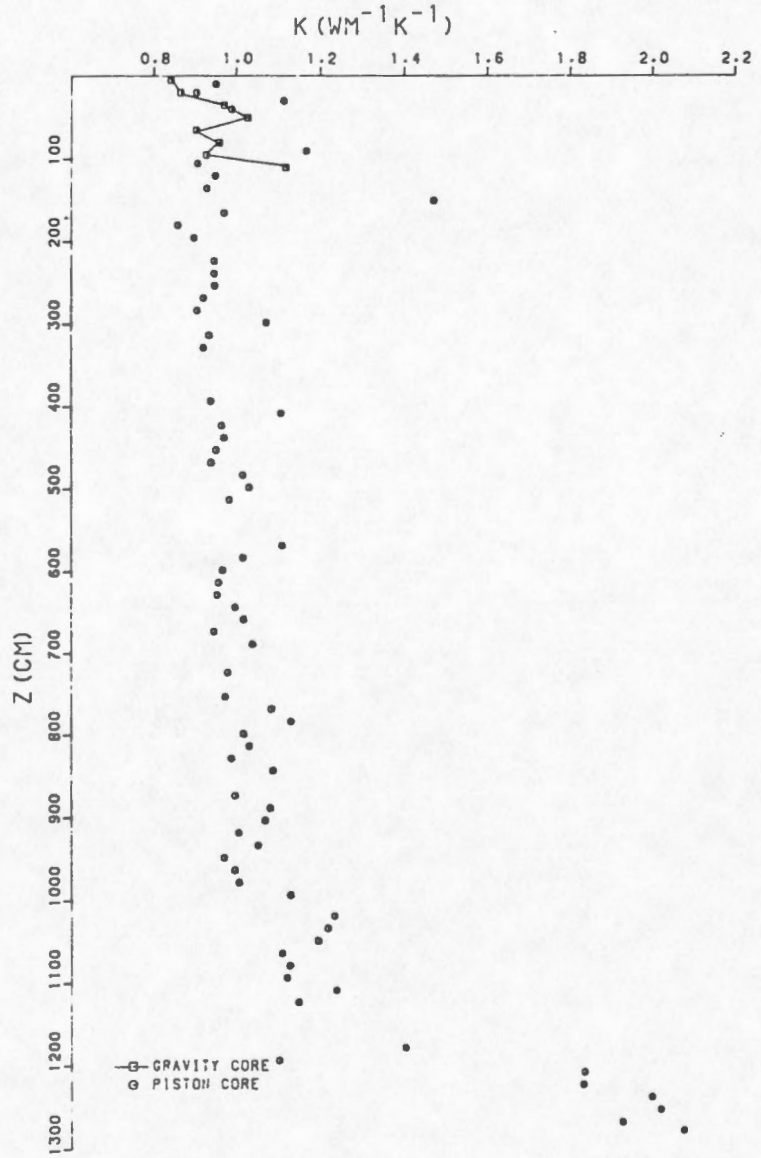

STATION 50, HUDSON 80-016, 32 32.05N, 55 58.61W

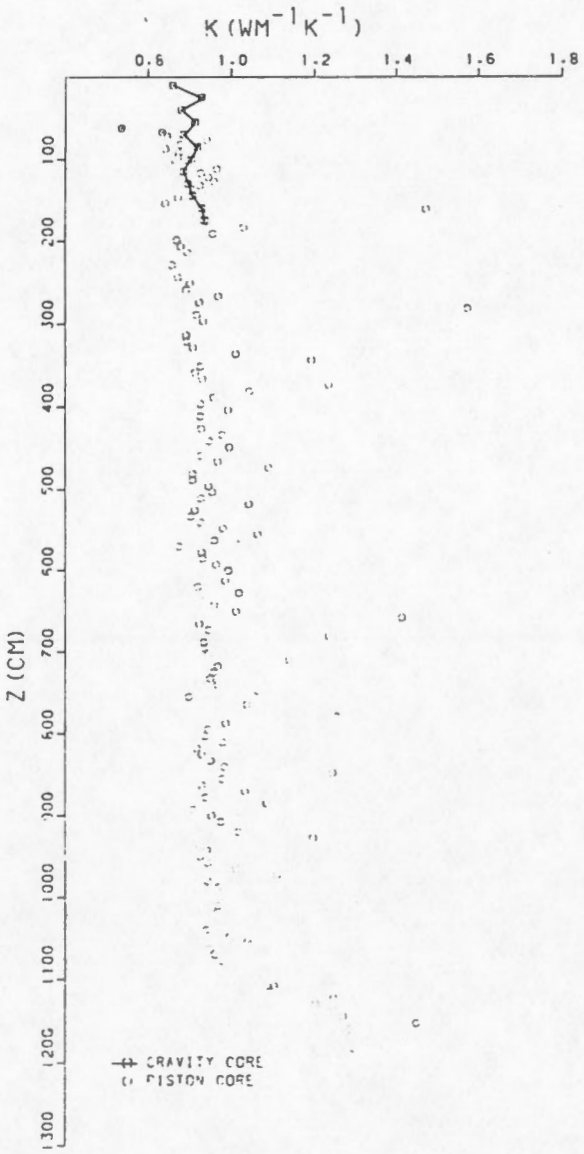

STATION 53 32 30.91N 55 59.19W

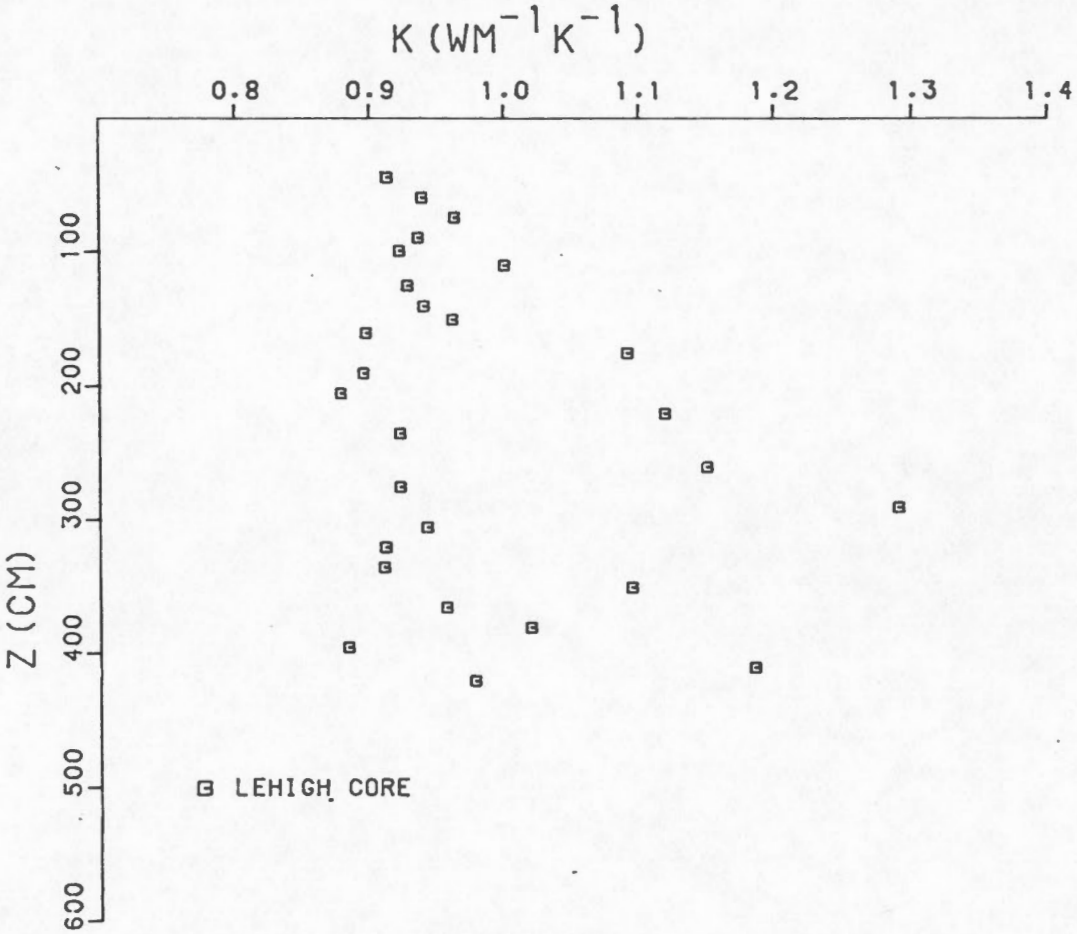

APPENDIX C

TEMPERATURE PROFILES AND BULLARD PLOTS

HUDSON CRUISE 80-016

SOHM ABYSSAL PLAIN

TEMPERATURE GRADIENTS

(calculated from a least squares fit to all temperature points on the T vs depth plot).

STATION	GRADIENT (mKm^{-1})	CORRELATION COEFF. R^2
26	55.6 ± 6.4	.997
35	35.0 ± 6.7	.996
38	53.0 ± 4.9	.999
41	68.4 ±12.4	.998
44-1	59.6 ± 9.2	.998
44-2	54.6 ± 6.0	.998

HEAT FLOWS

(calculated from a least squares fit to all points on the Bullard plot).

STATION	HEAT FLOW (mWm^{-2})	CORR. COEFF. R^2
26	53.4 ± 10.0	.994
35	36.1 ± 5.6	.996
38	54.5 ± 3.1	.999
41	67.1 ± 11.4	.998
44-1	57.9 ± 9.8	.998
44-2	52.9 ± 6.7	.998

STATION 26. HUDSON 80-016

32 30.99 N 55 56.92 W/O

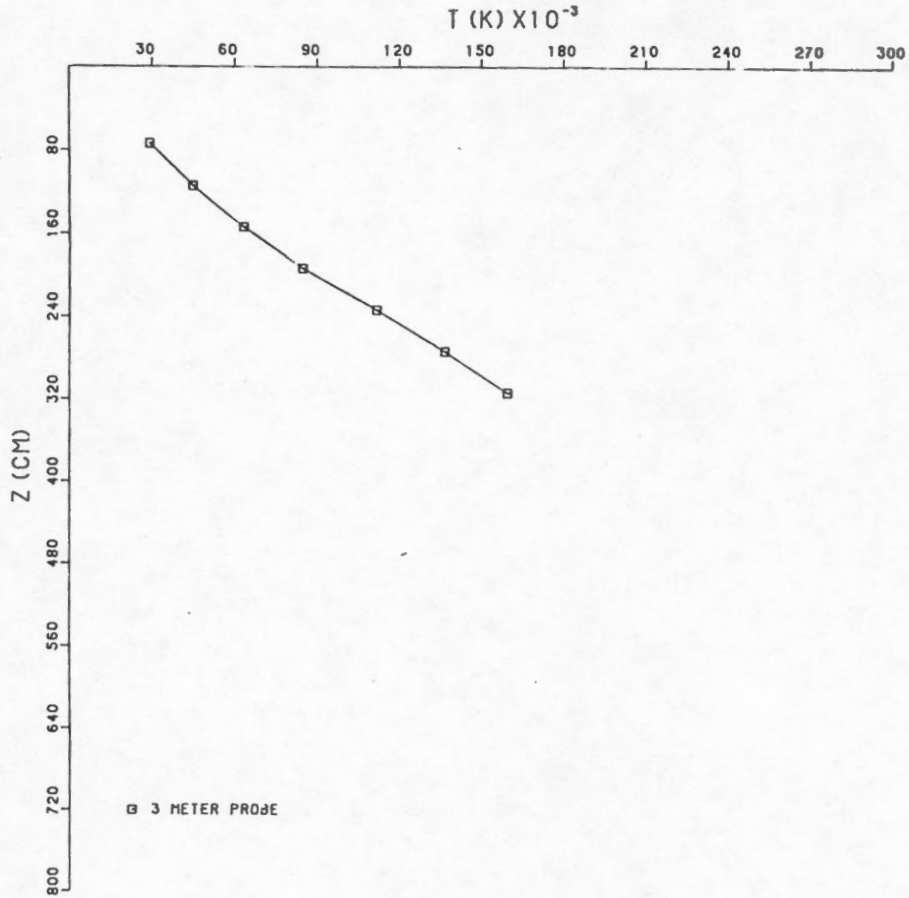

STATION 26. HUDSON 80-016

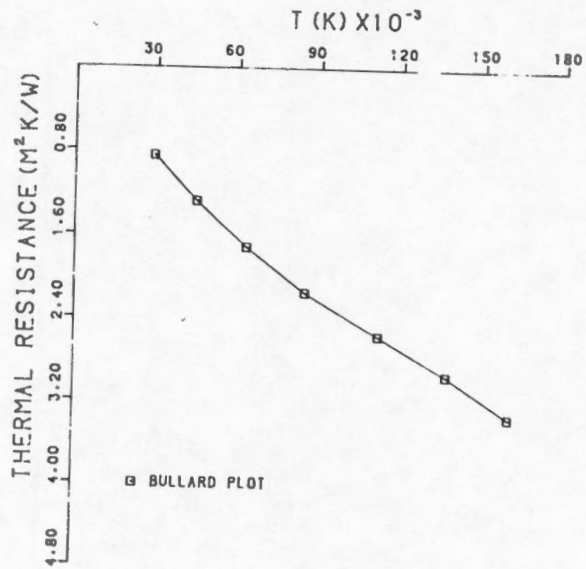

STATION 35. HUDSON 80-016

32 30.91 N 56 1.03 W/O

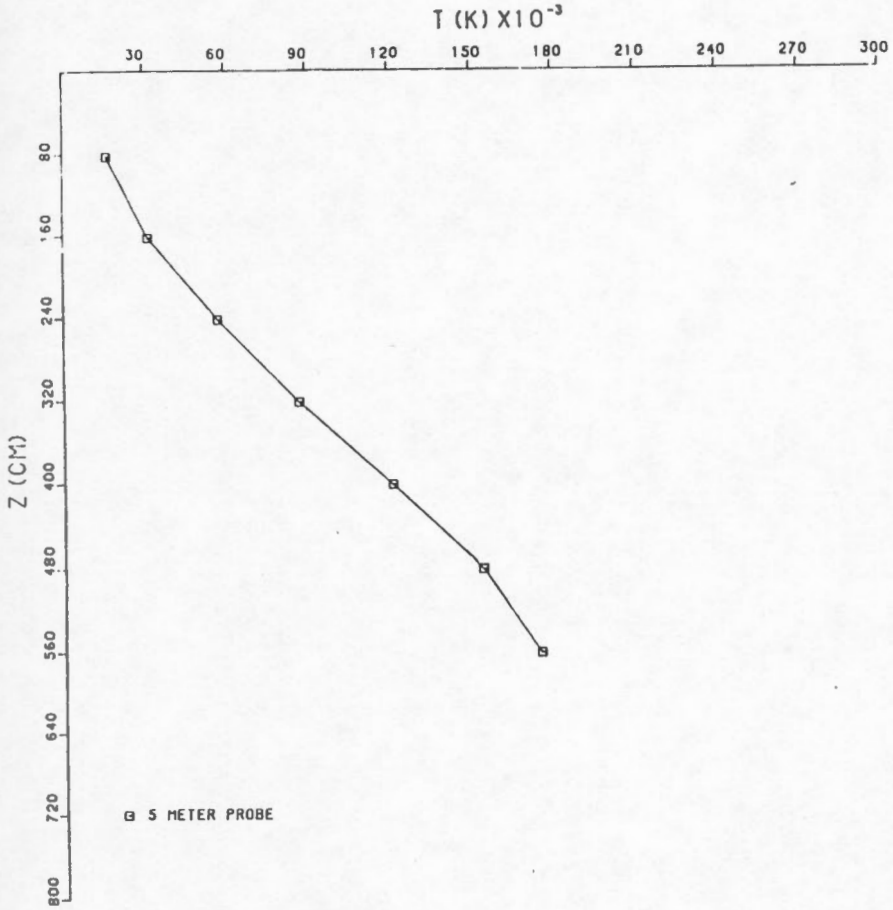

STATION 35. HUDSON 80-016

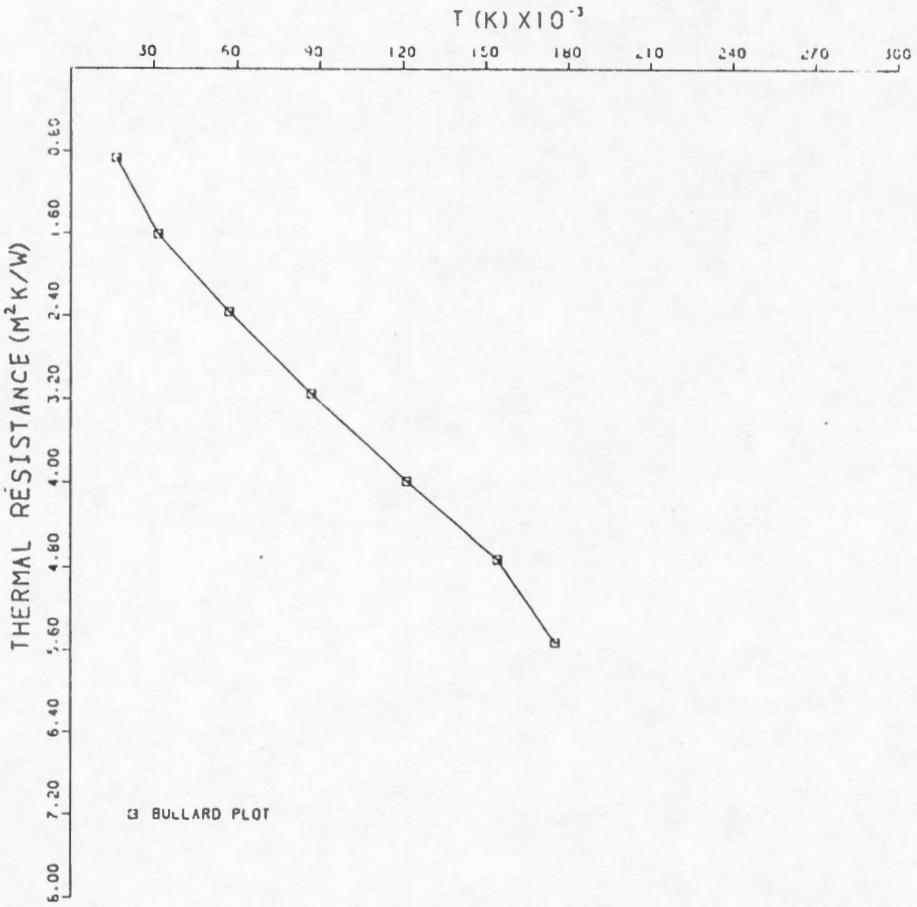

STATION 38. HUDSON 80-016

32 28.69 N 56 1.51 W/O

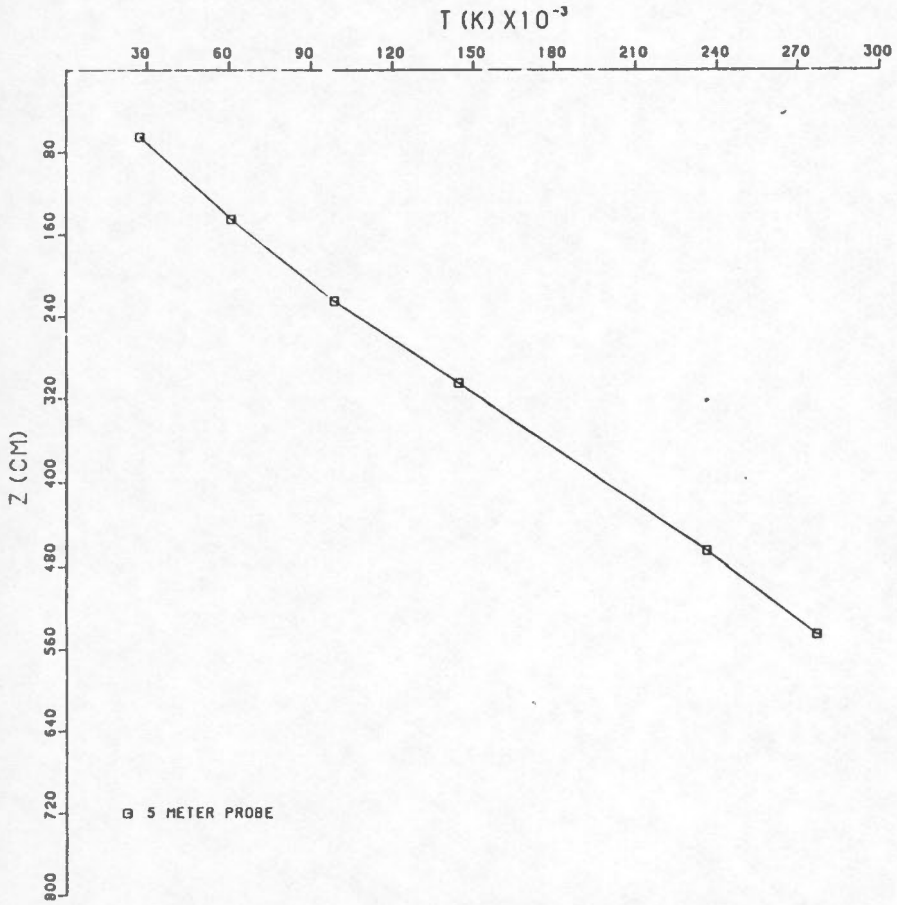

STATION 38. HUDSON 80-016

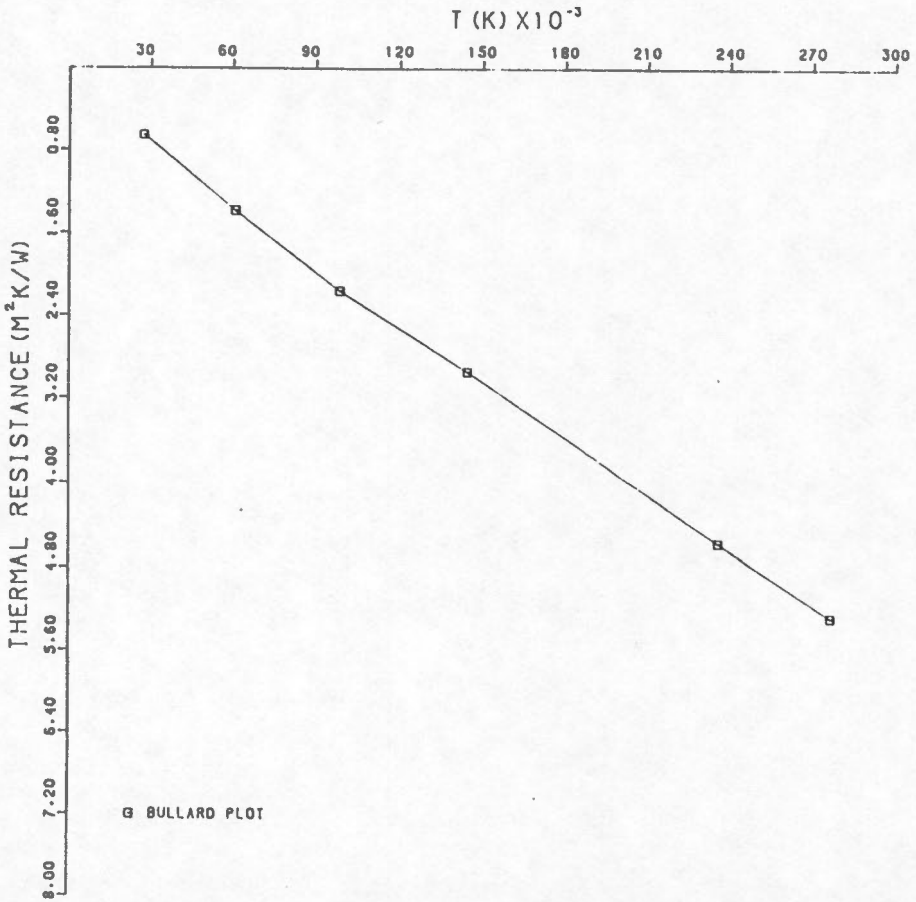

STATION 41. HUDSON 80-016

32 28.51 N 55 56.37 W/O

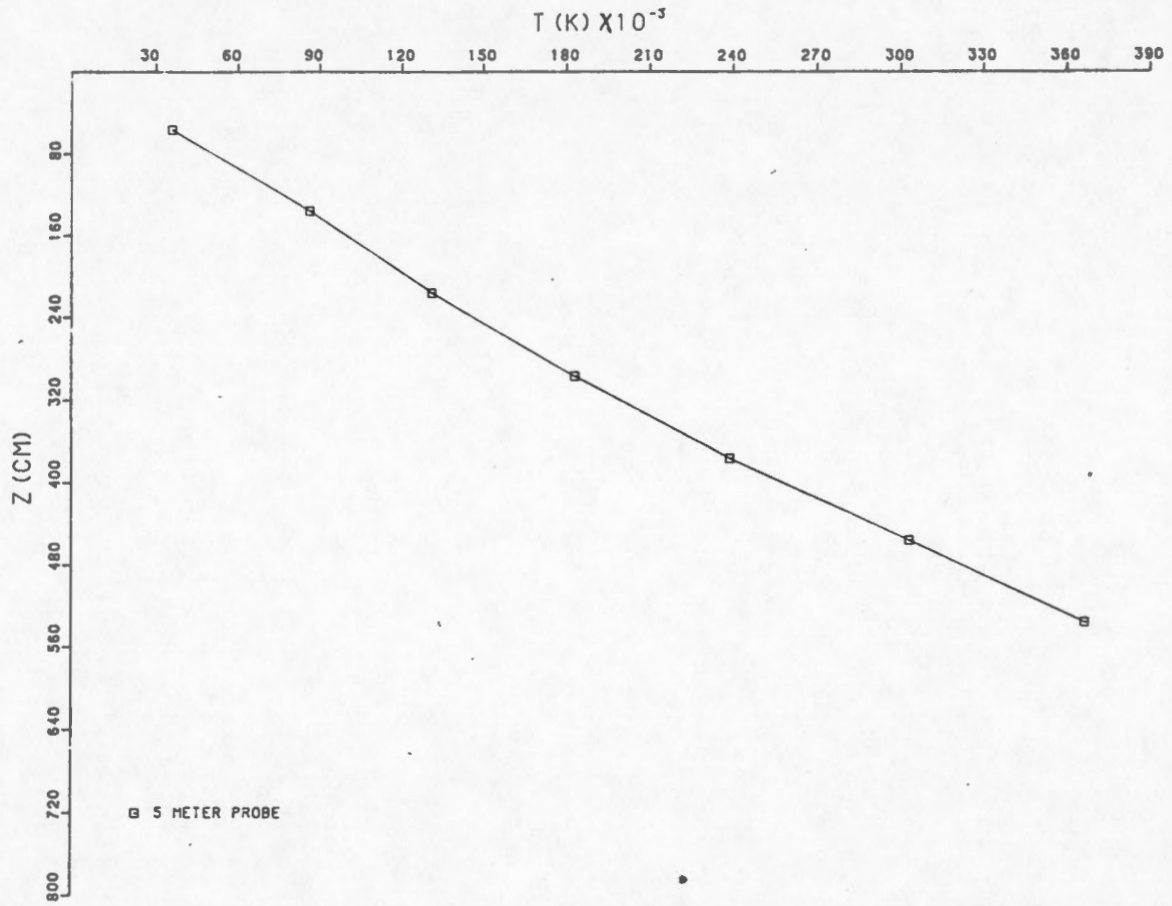

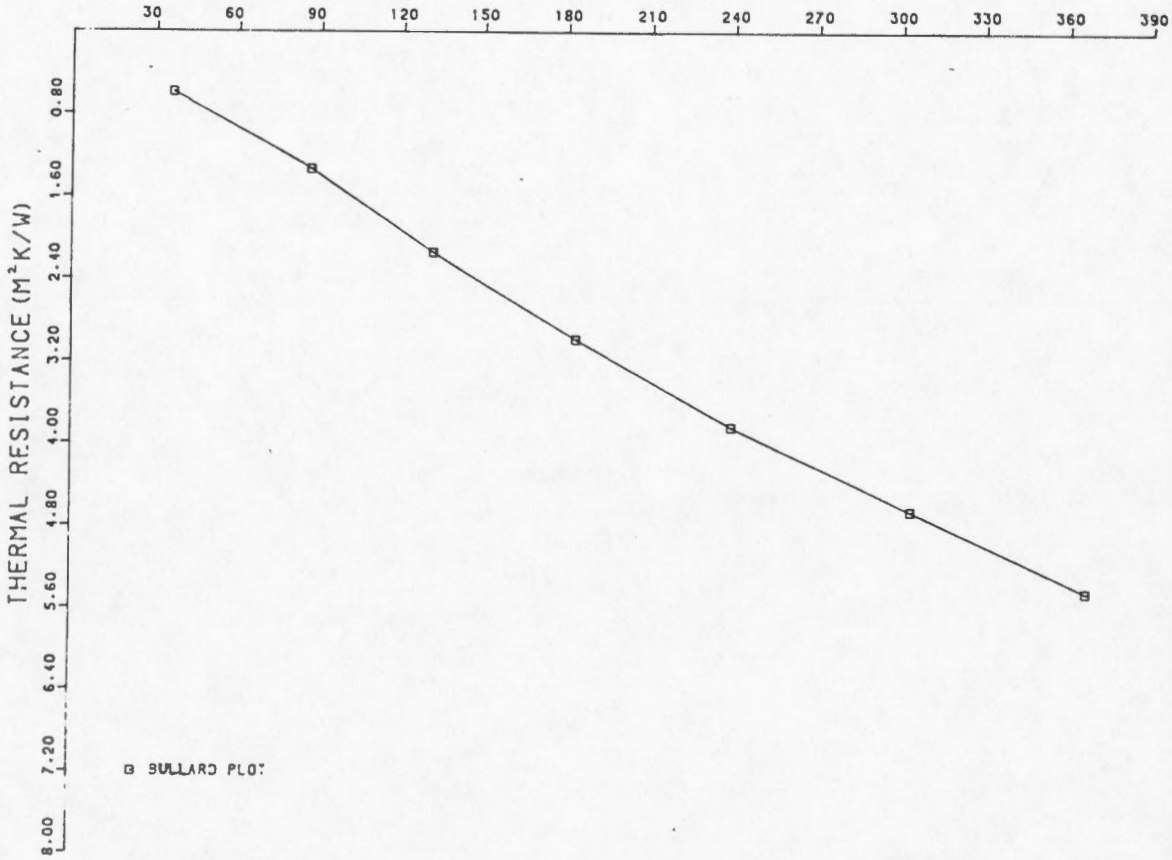

STATION 44-1, HUDSON 80-016

32 29.85 N 55 56.33 W/O

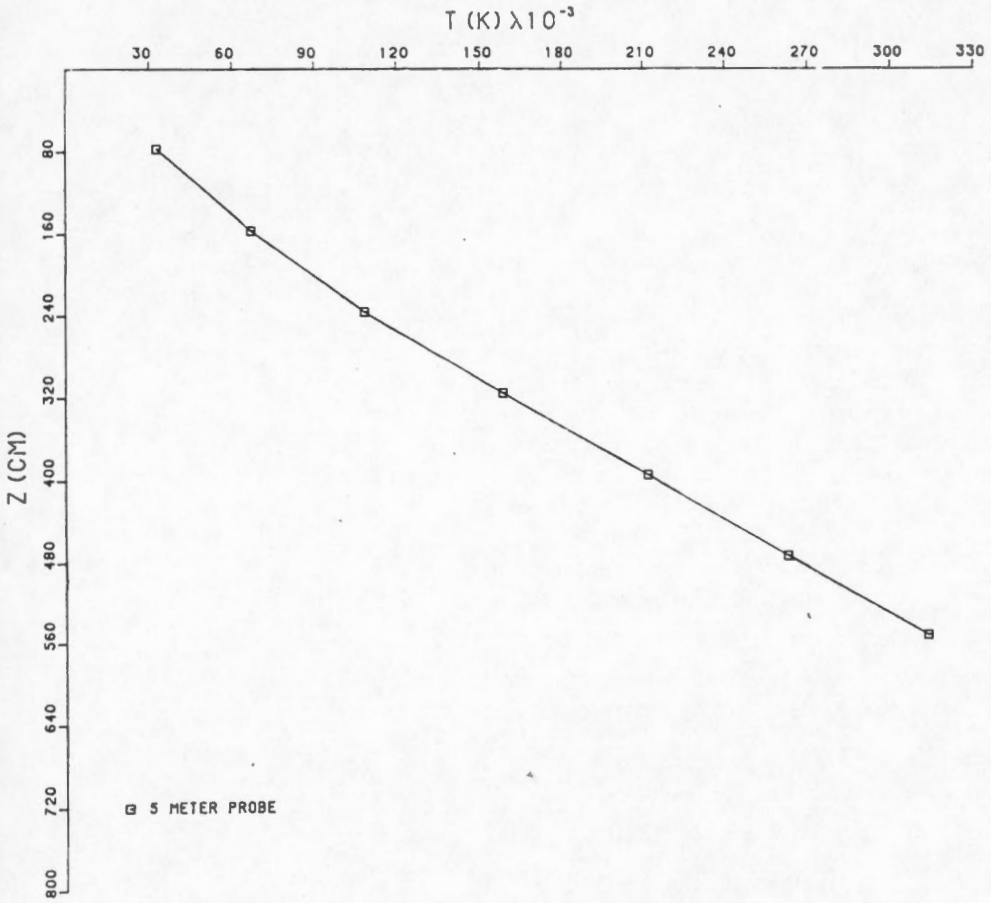

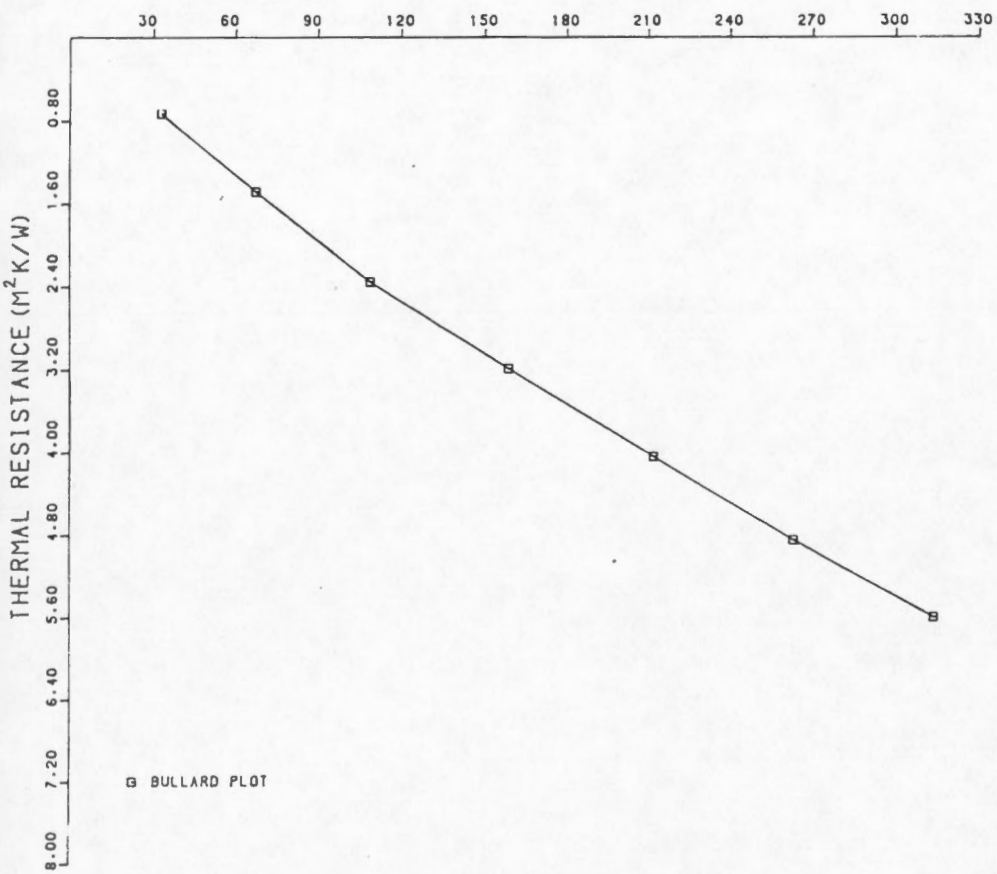

STATION 44-2. HUDSON 80-016

32 30.29 N 55 56.26 W/O